Summer 2015

Estimation of tip-sample force in tapping mode atomic force microscopy using neural-network and repetitive control approaches

Alireza Toghraee

Department:

ESTIMATION OF TIP-SAMPLE FORCE IN TAPPING MODE ATOMIC FORCE MICROSCOPY USING NEURAL-NETWORK AND REPETITIVE CONTROL APPROACHES

by

ALIREZA TOGHRAEE

A THESIS

Presented to the Faculty of the Graduate School of the

MISSOURI UNIVERSITY OF SCIENCE AND TECHNOLOGY

In Partial Fulfillment of the Requirements for the Degree

MASTER OF SCIENCE IN MECHANICAL ENGINEERING

2015

Approved by
Douglas A. Bristow, Advisor
S. N. Balakrishnan
Robert G. Landers

PUBLICATION DISSERTATION OPTION

This dissertation consists of the following two papers, formatted in the style used by the Missouri University of Science and Technology, listed as follows:

Paper 1 (pages 9-28), Alireza Toghraee, Douglas A. Bristow and S. N. Balakrishnan. “Estimation of tip-sample interaction in tapping mode AFM using neural-network approach,” American Control Conference, 2012, pp. 3222-3227.

Paper 2 (pages 29-55), Alireza Toghraee, Douglas A. Bristow, “Estimation of tip-sample force signal in tapping mode AFM using a repetitive control based filter,” under submission.

ABSTRACT

Atomic Force Microscopy is one of the most powerful tools for imaging, measuring and manipulating materials at nanometer scale. Among different modes of AFM, tapping mode, in which the oscillating tip touches the sample periodically, is most common mode. During the tip approach and retract, the tip interacts with sample and experiences different force regimes. This tip-sample interaction force contains information about the sample topology, material properties and tip geometry. However, quantitative measurement of the time-varying tip-sample interaction forcing function is challenging in the tapping mode because of the combined dynamic complexities of the cantilever and nonlinear complexity of the tip-sample force.

In first part of this research, an initial investigation of a neural-network approach to tip-sample interaction force estimation is studied. The tip-sample interaction is treated as an unknown force and a neural-network is used in a dynamic observer framework to approximate the unknown forcing function. Simulations are used to demonstrate plausibility of the approach and accuracy of the force model is evaluated for several scenarios.

In second part, an approach based on repetitive control is used to design a filter for execrating tip-sample force signal from noisy tip displacement measurements. Design of the filter parts and their parameters are explained and effect of each parameter on force estimation performance is discussed using simulations. Improvement in filter performance by using torsional harmonic cantilevers as the sensor is demonstrated.

ACKNOWLEDGMENTS

This would not have been done without helps and supports of many people. Here I would like to take this chance and thank them for their devoted help, time, and love.

First, I would like to thank my advisor Dr. Douglas Bristow who without his helps and ideas these works would not have been done. I would like to specifically thank him for being patient with me and for all his efforts to guide me through different steps and I wish we could have achieved more. I also would like to express my gratitude to my other committee members Dr. S. N. Balakrishnan for his great helps and hints and Dr. Robert Landers for his invaluable supports during my study.

Next, I would like to express my thanks to all my friends for their being beside me during all these years and for their priceless helps. Although names and memories of all them will be always in my mind, I would like to name Dr. Mohammad A. Alibakhshi, Mr. Hassan Golpour, Dr. Sajjad Ale Mohammadi, Mr. Kossha Marashi, and Hessam Zomorrodi for motivating and encouraging me and for keeping hope alive in my heart.

Finally yet importantly, I would like to thank my family; my mother for her unconditional love, my father for his encouragement and support during all my studies until now and my sister Negar whose smiles, even though from far, made spending all these years far from home easier. This work is dedicated to all of them.

TABLE OF CONTENT

Page

LIST OF ILLUSTRATIONS

LIST OF TABLES

1. INTRODUCTION

1.1 ATOMIC FORCE MICROSCOPY BACKGROUND

The atomic force microscopy (AFM) is now an advanced and useful method for direct measurements with atomic-resolution and can be employed in a broad spectrum of applications. The applications of atomic force microscopy can be divided in three main areas of imaging, measuring properties and manipulating small structures which are all done at the nanometer scale. Having the capability of measurement and manipulation at atomic scale, nowadays atomic force microscopes are used in various areas such as semi-conductors, materials, nanomechanics, polymers, biology and biomaterials [1]. AFM methods provide additional capabilities and advantageous relative to other microscopic methods (e.g., scanning electron microscopy (SEM) and transmission electron microscopy (TEM)). While SEM and TEM provide 2D images for conductive samples, 3D topography of semiconductors and biological samples in air or liquid medium can be obtained using AFM [2], [3]. Using AFM, high resolution imaging of DNA, proteins along with semiconductor and insulator surfaces have been acquired [4].

The main component of a typical AFM system is a micro-cantilever probe. One end of the cantilever is clamped to a support, which can be excited by a piezoelectric (PZT) actuator, and the other end which has a sharp tip is in interaction with. Movement of the tip is obtained by a sensitive photo detector which senses a laser beam reflected back from the free end of the cantilever. Deflection and rotation of the tip changes the position of the reflected laser beam on the photo detector. These changes are transformed to electrical signals forming feedback measurements (Figure 1.1). The principle of AFM operation is to make the tip scanning the sample contour by moving the sample under the tip while maintaining tip and sample interaction. Interatomic interaction between tip and sample is a function of their distance from each other and tip will experience different regime as tip-sample separation changes. When the separation is high, there is very weak attractive force between tip and sample. As tip approaches the sample, attractive forces increase until tip and sample are so close that electron clouds start to repel each other electrostatically. The interaction force becomes zero when separation is a couple of Angstroms and becomes highly repulsive when tip and sample are in contact.

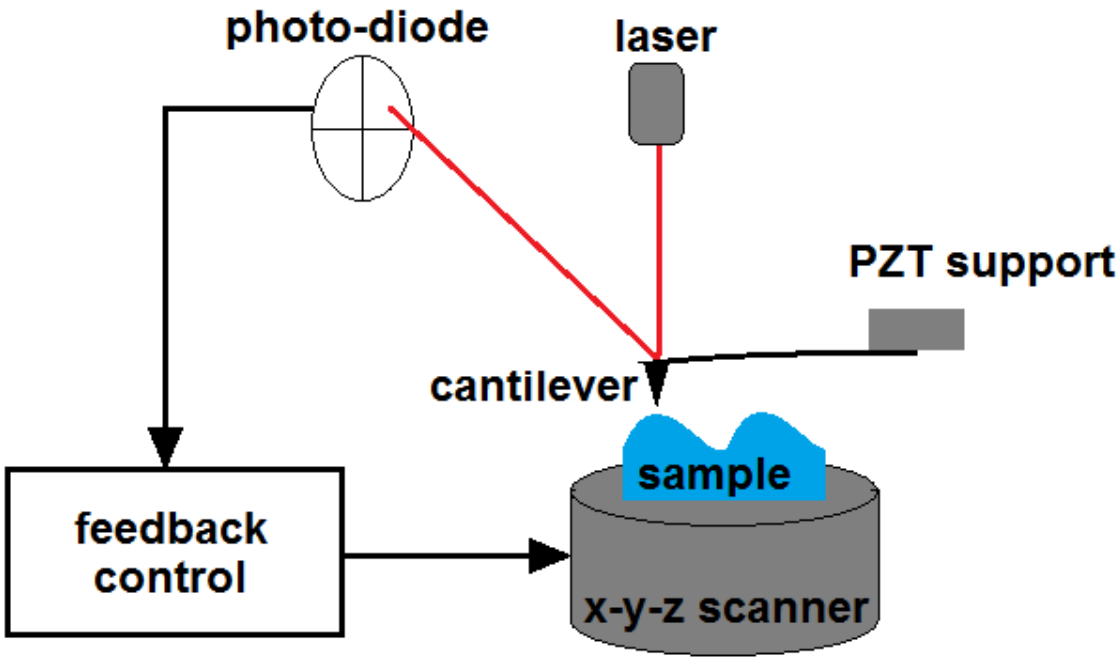

Figure 1.1 Schematic of an AFM.

Different modes of AFM are determined basically by the regime in which the it is operated. In contact mode the tip is operated in repulsive regime of the interaction force and tip is in very close contact with sample. Surface topography of sample is generated by operating in constant height mode or constant force mode. In constant height mode, the probe scans the sample without moving in z-direction. Thus, cantilever deflection resulted from repulsive forces can be used to generate surface image. In constant force mode, a piezoelectric element (PZT) is used to move sample or probe such that the normal force between tip and sample remains constant. At first, the cantilever is lowered to bring tip and sample in contact and this initial deflection of cantilever is recorded as a set point. As tip scans the sample cantilever deflection changes from initial state. This

difference is compared with the set point value and error signal is used to actuate the PZT element to bring cantilever to its initial condition. This error signal hence can be used to measure the surface profile. The drawback of contact mode this is that it cannot be applied on soft materials since shear and dragging forces generated during scanning will damage the soft sample (specifically biological ones) and hence distort the image [1].

The problems in contact mode are addressed in tapping mode which is one of the dynamic modes in AFM. In this mode, the cantilever is excited at a frequency near its resonant natural frequency using a PZT actuator at the support. When cantilever is far from the sample, there is no interaction force and cantilever tip oscillates at its free amplitude. When the tip is lowered, it starts to tap the surface lightly and will experience both attractive and repulsive regimes. Vibration amplitude of tip changes according to sample surface profile. If tip scans a bump on the sample, the amplitude will decrease due to lack of enough space. On the other hand, the amplitude will increase (up to free amplitude) as tip goes over a valley on the sample (Figure 1.2). During tapping mode operation, it is tried to keep oscillation amplitude constant using feedback control. The change is amplitude is sensed by optical sensor and fed back to control system. This amplitude is then compared with the set point value and the error signal is used to actuate the PZT element in the z-direction to adjust the tip-sample distance such that oscillation amplitude remains constant. This error signal which is related to sample topography is used to generate the image.

1.2 TIP-SAMPLE FORCE IMPORTANCE AND METHODS TO ESTIMATE THAT

Dynamic modes of operation in AFM are challenging since cantilever tip experiences various force regimes with different intensity in a short period of time. These complex forces may result in different stable trajectories cantilever or even chaotic behavior under certain operation conditions and set points [5]. Thus, understanding tip-sample force profile is of great importance for stable high resolution imaging particularly for non-contact mode which operates the cantilever mostly on attractive regime [6]. In addition, having information about tip-sample force profile will result in design of high performance controllers which lead to faster scanning with lower measurement errors [7].

Furthermore, tip-sample interactions are related to tip and sample material, charge, chemistry and geometry [8], [9] and extracting tip-sample force information can be used for material identification and determining tip damage and wearing [10], [11].

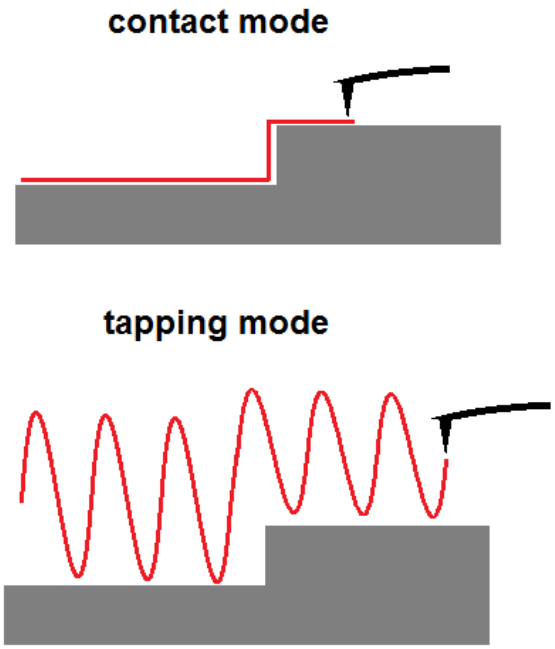

Figure 1.2 Comparison of cantilever tip trajectory in contact and tapping mode AFM.

Many methods have been developed to obtain information on tip-sample interaction profile. Most of methods to determine these forces in tapping mode AFM are based on the fact that the amplitude, frequency and phase shift of the tip oscillation relate the cantilever dynamic to tip-sample interaction and they can be used to track back the sample topography and its interaction with tip. In one method, phase shift of the cantilever motion is used to determine the operating regime (attractive or repulsive) of tip [12]. Change of resonance frequency as function of resonance amplitude is used in other

approaches to create the tip-sample force function in high vacuum [13], [14]. This method is further improved to measure the force in the ambient condition also [15]. Another approach designs a torsional harmonic cantilever (THC) to couple tip-sample interactions with rotation in the probe [16], [17]. Many of the mentioned methods in tapping mode AFM use steady-state response of the tip to calculate tip-sample force. Although steady-state measurements simplifies correlation between cantilever and force and reduces sensitivity to noise, they cannot be efficient in practice due to slow response of probes with high quality factors [18]. In one non-steady-state method [19] uses an inverse dynamic model of the cantilever to reconstruct tip-sample forces from displacement measurements. However, direct dynamic inversion has a downfall of sensitivity to noise and uncertainty in the model.

1.3 RESEARCH OBJECTIVE

Objective of this research, which is presented in two papers, is to explore methods to extract tip-sample force signal and profile from measured cantilever displacement. These methods can be used and implemented in real-time to provide tip-sample force profile and map the estimated force to the captured image.

In first paper, a Neural-Network (NN) approach is used for force estimation since they are known for their ability to approximate complex unknown functions. This will result in obtaining tip-sample force curves that can be used in design of high-performance adaptive controllers and material identification. Using the method developed in [20], the Neural-Network force estimator is evaluated in simulation using simple models for cantilever dynamics and tip-sample force. Effectiveness and ability of the technique is demonstrated by considering different scenarios.

In second paper, a method based on repetitive control (RC) is developed to reconstruct the tip-sample force signal. RC method is used since it is well-known to deal with systems having periodic references and disturbances [21], [22] and also they can address the problem of noise in the measurements. The goal in this part is using simulations to evaluate the performance of the presented RC based filter to extract tip-sample force. In addition, considering advantages of utilizing higher harmonics in AFM

[23], [24], a solution based on torsional cantilever model is suggested to improve RC method performance.

REFERENCES

[1] N. Jalili, K. Laxminarayana, “A review of atomic force microscopy imaging systems: application to molecular metrology and biological sciences,” Mechatronics, vol. 14, 2004, pp. 907-945.

[2] S. M. Salapaka, M.V. Salapaka, “Scanning probe microscopy,” IEEE control system magazine, 2008, pp. 65-83.

[3] H.N. Pishkenari, N. Jalili, A. Meghdari, “Acquisition of high-precision images for non-contact atomic force microscopy,” Machatronics, vol. 16, 2006, pp. 655-664.

[4] R. Garcia, R. Perez, “Dynamic atomic force microscopy methods,” Surface Science Reports, vol. 47, 2002, pp. 197-301.

[5] A. Sebastian, A. Gannepalli, M.V. Salapaka, “A review of the systems approach to the analysis of dynamics-mode atomic force microscopy,” IEEE transactions on control systems technology. vol. 15, 2007, pp. 952-959.

[6] N. Jalili, M. Dadfarnia, D.M. Dawson, “A fresh insight into the microcantilever-sample interaction problem in non-contact atomic force microscopy” Journal of Dynamic Systems, Measurement and Control, vol. 126, 2004, pp.327-335.

[7] G. Schitter, P. Menold, H. F. Knapp, F. Allgowerb, A. Stemmer, “High performance feedback for fast scanning atomic force microscopes,” Review of Scientific Instruments, vol. 72, 2001, pp. 3320-3327.

[8] J.N. Israelachvili, Intermolecular and Surface Forces, Academic Press, 2nd ed., 1991.

[9] E. Bonaccurso, F. Schönfeld, H.J. Butt, “Electrostatic forces acting on tip and cantilever in atomic force microscopy,” Physical Review B vol. 74, 2006, pp. 085413.

[10] S. Crittenden, A. Raman, R. Reifenberger, “Probing attractive forces at the nanoscale using higher-harmonic dynamic force microscopy,” Physical Review B, vol. 72, 2005, pp. 1-13.

[11] S. Hu, S. Howell, A. Raman, R. Reifenberger, M. Franchek. “Frequency domain identification of tip-sample van der Waals interactions in resonant atomic force micro cantilevers,” Journal of Vibration and Acoustics, vol. 126, 2004, pp. 343-351.

[12] R. Garcia, A. San Paulo, “Attractive and repulsive interaction regimes in tapping-mode atomic force microscopy,” Physical Review B, vol. 60, 1999, pp. 4961-4967.

[13] H. Holscher, W. Allers, U. D. Schwartz, R. Wiesendanger, “Determination of tip-sample interaction potentials by dynamic force spectroscopy” Physical Review Letters, vol. 83, 1999, pp. 4780-4783.

[14] B. Gotsmann, B. Anczykowski, C. Seidel, H. Fuchs, “Determination of tip-sample interaction forces from measured dynamic force spectroscopy curves,” Applied Surface Science, vol. 140, 1999, pp. 314-319.

[15] H. Holscher, W. Allers, U. D. Schwartz, R. Wiesendanger, “Determination of tip-sample interaction potentials by dynamic force spectroscopy,” Physical Review Letters, vol. 83, 1999, pp. 4780-4783.

[16] O. Sahin, S. Magonov, C. Su, C. F. Quate, O. Solgaard, “An atomic force microscope tip designed to measure time-varying nanomechanical forces,” Nature Nanotechnology, vol. 2, 2007, pp. 507-513.

[17] O. Sahin, “Time-varying tip-sample force measurements and steady-state dynamics in tapping-mode atomic force microscopy,” Physical Review B, vol. 77, 2008, art. No. 115405.

[18] D. R. Sahoo, A. Sebastian, M. V. Salapaka, “Harnessing the transient signals in atomic force microscopy,” International Journal of Robust Nonlinear Control, vol.15, 2005, pp. 805–820.

[19] M. Stark, R. W. Stark, W. M. Heckl, R. Guckenberger. “Inverting dynamic force microscopy: from signals to time-resolved interaction forces,” Applied Physical Sciences, vol. 99, No. 13, 2002, pp. 8473-8478.

[20] R. Padhi, N. Unnikrishnan, S.N. Balakrishnan, “Model-following neuro-adaptive control design for non-square, non-affine nonlinear systems,” IET Control Theory Appl., vol. 1, 2007, pp. 1650-1661.

[21] R. W. Longman, “Iterative learning and repetitive control for engineering practice,” International Journal of Control, vol. 73, No. 10, 200, pp. 930-954.

[22] M. Steinnuch, “Repetitive control for systems with uncertain period-time,” Automatica, vol. 38, 2002, pp. 2103-2109.

[23] M. Loganathan, D. A. Bristow, “Bi-harmonic cantilever design for improved measurement sensitivity in tapping-mode atomic force microscopy,” Review of Scientific Instruments, vol. 85, 2014, pp. 043703.

[24] S. Sadewasser, G. Villanueva, J. A. Plaza, “Modified atomic force microscopy cantilever design to facilitate access of higher modes of oscillation,” Review of Scientific Instruments, vol. 77, 2006, pp. 073703.

PAPER

I. ESTIMATION OF TIP-SAMPLE INTERACTION IN TAPPING MODE AFM USING NEURAL-NETWORK APPROACH

ABSTRACT

In Atomic Force Microscopy, the tip-sample interaction force contains information about the sample topology, material properties and tip geometry. However, quantitative measurement of the time-varying tip-sample interaction forcing function is challenging in the tapping mode because of the combined dynamic complexities of the cantilever and nonlinear complexity of the tip-sample force. In this paper, an initial investigation of a neural-network approach to tip-sample interaction force estimation is studied. The tip-sample interaction is treated as an unknown position-dependent force on the cantilever. A modified radial basis function neural-network is used in a dynamic observer framework to approximate the unknown forcing function. Design of the observer gains is discussed and simulations are used to demonstrate plausibility of the approach. Accuracy of the force model is evaluated for several different tip-sample distances and materials and future direction are discussed.

1. INTRODUCTION

The atomic force microscope (AFM) is an important tool for imaging, measuring and manipulating small structures at the nanoscale. In particular, the AFM is a powerful tool for measuring sample topography and mechanical properties with atomic resolution [1]-[5]. When the tip of the AFM probe approaches the sample, atomic forces, such as van der Waals force, act on the tip affecting the motion of the AFM probe, which is detected, typically by an optical lever. The tip-sample forces depend on many parameters including the distance of the tip-sample separation, tip and sample materials, charge, chemistry, and tip geometry [6],[7]. Thus, the tip-sample forcing function contains a great deal of information about the sample and state of the probe. This information can be useful for high-performance controllers [8],[9] and better imaging [10], sample material identification [11],[12], and determining tip damage or contamination.

Many methods have been developed for extracting tip-sample force information. Many of the methods relevant to the tapping AFM mode are based on steady-state response of the probe. The steady-state simplifies the correlation between the detected motion and the tip-sample force, but can be inefficient or inaccurate in practice due to the slow response of high-Q probes. In one method, the steady-state phase shift of the probe's oscillation is used to determine if the probe is in the repulsive region, very near the sample [13]. A "bimodal" imaging mode [14] excites the probe at its second resonance and uses the second resonance phase shift to determine material stiffness. In [15]-[17] amplitude and phase are measured as the tip-to-sample offset is varied to create a map of the tip-sample force. Another approach utilizes a torsional harmonic cantilever to couple tip-sample forces to rotation in the probe [18], [19]. One non-steady-state method [20] uses an inverse dynamic model of the probe to construct tip-sample force estimates from displacement measurements. However, direct dynamic inversion is well known to be very sensitive to measurement noise and model accuracy and can be computationally expensive. Another non-steady-state method [10] constructs a nonlinear estimator to obtain the time-varying offset between the tip and sample.

In this paper, we explore a method to obtain a model of the time-varying tip-sample force from the measured probe displacement. The model can be used for development of high-performance adaptive controllers and measurement of the sample topography and material properties. Our approach utilizes a Neural-Network (NN) model because NNs are known for their ability to model complex and unknown functions, they have been successfully demonstrated in a wide variety of applications, and they can be solved in parallel, which is critical for real-time implementation [21], [22]. The objective of this paper is to evaluate the NN technique in simulation using simple models of the probe dynamics and tip-sample forces in order to determine potential efficacy for the AFM problem as well as identify key areas for future research and development.

The rest of article is organized as follows. In section 2, an AFM model is presented. The neural-network based estimator is introduced in section 3 which uses the simulated states from AFM as input and provides an estimation of tip-sample force as output. In Section 4 a variety of scenarios are studied in simulation to determine efficacy of the proposed approach. Conclusions are given in section 5.

2. AFM MODELING

The AFM dynamics are commonly modeled as a SDOF spring-mass-damper system [1],[8],[10],[23]. Using this model, the equation of motions which represent the tip position can be written as,

$$m\ddot{x}(t) + c\dot{x}(t) + kx(t) = F_{dr}(t) + F_{ts}(x), \tag{1}$$

where m is the equivalent cantilever-tip mass, c is the equivalent viscous damping and k is the equivalent cantilever spring constant. x is the tip position and measured from the rest position (Figure 2.1). $F_{dr}(t)$ is the driving force which is typically from position excitation, $u_{dr}(t)$, of piezo mounted at the base of the cantilever and can be represented by,

$$F_{dr}(t) = c\dot{u}(t) + ku(t), \tag{2}$$

and the $F_{ts}(x)$ is the tip-sample interaction force. For easier analysis and simulation, it is standard to normalize the dynamics using the dimensionless parameter $\tau = t\omega$, where $\omega = \sqrt{k/m}$ is the natural frequency [23]. Defining the quality factor as $Q = m\omega/c$, (1) can be written as,

$$\ddot{x}(\tau) + \frac{1}{Q}\dot{x}(\tau) + x(\tau) = \frac{1}{Q}\dot{u}(\tau) + u(\tau) + \frac{F_{ts}(x)}{k}. \tag{3}$$

There are different types of forces such as electrostatic and Van der Waals forces acting on an AFM tip [7],[9],[24],[25]. These forces are generally dependent on various parameters like tip-sample separation, sample material, tip configuration, etc. Different mathematical models such as Derjaguin-Muller-Toporov (DMT) [23] and Lennard-Jones [6],[24] have been used to represent the tip-sample interaction force and worked well to simulate/control the AFM [9]. Here, for the purposes of this work, it will be assumed that

the interaction force is based on the Lennard-Jones model [6],[24]. According to this model, the tip-sample force is given by,

$$F_{ts}(x) = +\frac{A_1 R}{180(x+x_s)^8} - \frac{A_2 R}{6(x+x_s)^2}, \tag{1}$$

where the coefficients A_1, A_2 are the Hamaker constants of intermolecular pair potential for the tip and sample [24]. The gap between the sample and the nominal position of the tip (when x=0) is x_s and R is the tip radius. The drive force F_{dr} is typically a sine wave near the resonant frequency of cantilever. Using, (3), and considering base excitation $u_{dr}(t)$, and $F_{ts}(x)$ as inputs, the state-space model of the AFM can be obtained as follows,

$$\begin{aligned} \dot{X} &= A\,X + B_{dr}u_{dr}(\tau) + B_{ts}F_{ts}(x_1) \\ X &= \begin{bmatrix} x_1 \\ x_2 \end{bmatrix}, A = \begin{bmatrix} \frac{-1}{Q} & 1 \\ -1 & 0 \end{bmatrix}, B_{dr} = \begin{bmatrix} 1 \\ \frac{1}{Q} \end{bmatrix}, B_{ts} = \begin{bmatrix} 0 \\ \frac{1}{k} \end{bmatrix}, \end{aligned} \tag{2}$$

where $x_1 = x$, $x_2 = \dot{x}$ and differentiation is carried with respect to normalized time.

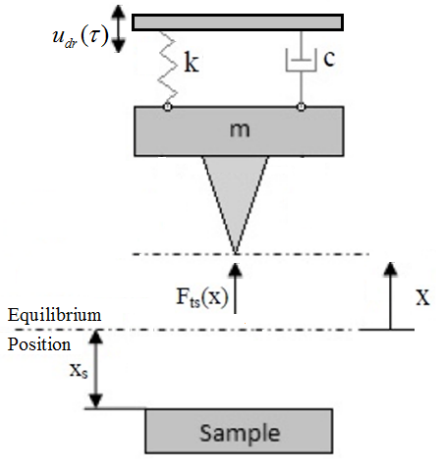

Figure 2.1 SDOF model of AFM.

3. NEURAL NETWORK BASED ESTIMATION

3.1 ESTIMATION PROCEDURE

The goal of the neural-network estimation is to construct a model for the unknown function F_{ts} in (5). According to the universal function approximation property of neural networks [26] this function can be reconstructed by a set of optimal weight vectors *W* and basis function vectors $\phi(x_1)$ with the accuracy level of ε, or,

$$F_{ts}(x_1) = W^T \phi(x_1) + \varepsilon \,. \tag{3}$$

By estimating weight vector *W* and eliminating the accuracy term the estimated unknown function $F_{ts}(x_1)$ is obtained as,

$$\hat{F}_{ts}(x_1) = \hat{W}^T \phi(x_1) \,, \tag{4}$$

where $\hat{W}$ is the estimated weight. Now, consider the observer model given by,

$$\dot{\hat{X}} = A\hat{X} + BF_{dr}(\tau) + B\hat{F}_{ts}(x_1) + K(X - \hat{X}) \,, \tag{5}$$

where $\hat{X}$ is the estimated state vector and *K* is the state-estimator gain. *K* can be chosen as a diagonal matrix with the inverse of time constants on its diagonal [21]. By defining the state-approximation-error as $e_a = X - \hat{X}$ and weight-approximation-error as $\tilde{W} = W - \hat{W}$, the state error dynamics can be expressed as,

$$\dot{e}_a = \tilde{W}^T \phi(x_1) + \varepsilon - Ke_a \,. \tag{6}$$

To ensure bounds on state error e_a and to also on the adaptive weight $\hat{W}$, the stabilizing weight update rule given by [21],

$$\dot{\hat{W}} = G\phi(x_1)e_a^T - G\sigma\hat{W} \,, \tag{7}$$

will be used, where $G \in R^{n \times n}$ and σ are the adaptation rate and modification factor respectively. Estimation based on this method is based on the assumption that measurements for both states (position and velocity) are available. Although velocity measurements are not typically available in AFMs they can be estimated through position measurements. This point is discussed further in the conclusions in Section 5.

3.2 RADIAL BASIS FUNCTION NETWORK (RBF)

Although it is well known that the type of basis function can play an important role in the effectiveness of the neural network estimator, generally, there is not a standard way to pick the best basis functions for a particular application. A good rule of thumb is to use basis functions that represent the nature of the unknown approximated function to some extent. Here we use the radial basis functions (RBFs)

$$RBF(z) = \exp\left(-\left(\frac{z-\delta}{\sigma_e}\right)^2\right), \tag{8}$$

where the parameters δ and σ_e in can be adjusted to select the RBF center and width, respectively. In the application considered in this paper, *z* represents the position *x*. Thus, key properties of the RBF, that it has smooth derivatives and is highly localized, match the expected tip-sample forces which are also smooth and occur only when the tip is very near the sample.

In the AFM problem, proper scaling of the RBF is critical since the range of motion of *x* is small (typically 10s of nanometers) and the tip-to-sample forces occur over an even smaller range (typically 1-3 nanometers). As a result, without care in the scaling and shifting the parameters in (11) one can expect that $RBF(x) \approx 1$, and so accurate estimation will require a large number of basis and may be sensitive to numerical errors. Proper scaling of the basis functions is therefore important. Furthermore, the slope of the repulse portion of the tip-to-sample force is significantly higher than the slopes in the attractive force region. Although it is possible to account for the variation with different RBF widths, we find that it is advantageous to also increase the power on the Gaussian function (11) to create a sharper peak. This is illustrated in Figure 2.2.

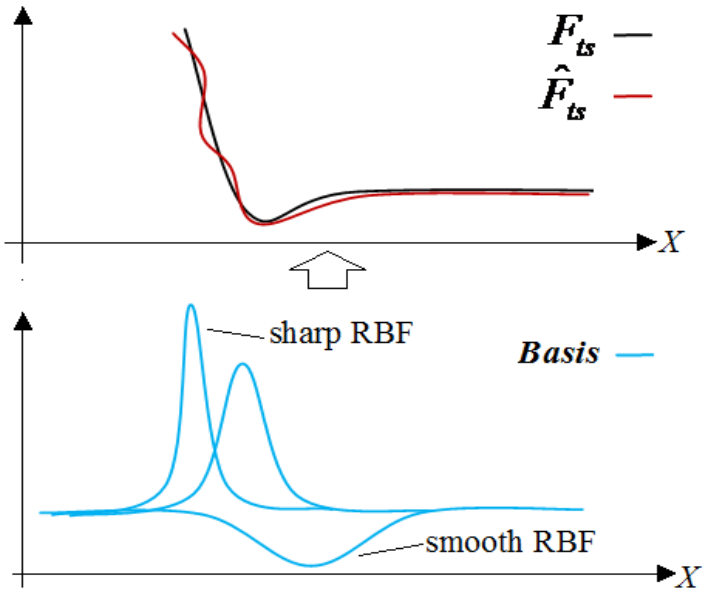

Figure 2.2 Schematic view of estimating a function by different basis functions.

The modified RBF set used here is given by,

$$RBF_{ij}(x) = \exp\left(-\left(\frac{x+\bar{x}+\delta_j}{\sigma_{e_i}}\right)^{p_i}\right), \tag{9}$$

which includes several offsets δ_j and sharpnesses $\left(\sigma_{e_i}, p_i\right)$. The constant $\bar{x}$ represents a best guess for the expected tip-to-sample distance where the force switches from attractive to repulsive. For Lennard-Jones model, the point at which the force switches from attractive to repulse in many materials is approximately 1nm from the offset, x_s. Therefore, for example, if the tip-to-offset distance is expected to be in the range 9nm to 10nm, and a spatial accuracy of 0.25nm is desired, then $\bar{x} = 8.5\text{nm}$ and $\delta_j = \{-0.5, -0.25, 0, 0.25, 0.5\}$ nm for j=1,…,5, respectively. For sharpness, we find that the combinations,

$$\left(\sigma_{e_i}, p_i\right) = \left\{\left(10^{-9}, 2\right), \left(2\times10^{-9}, 2\right), \left(0.75\times10^{-9}, 4\right), \left(0.5\times10^{-9}, 6\right)\right\} \quad (10)$$

for i=1,..,4, work well.

Combining the equations of Section 3.1 and 3.2, a block diagram of the neural network estimator is shown in Figure 2.3.

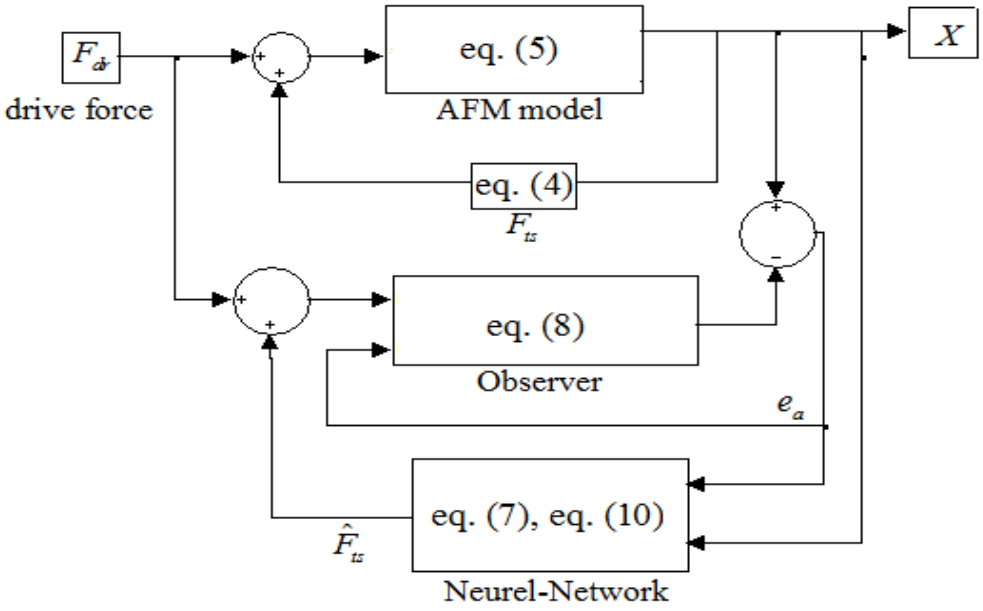

Figure 2.3 Schematic view of implemented system.

4. SIMULATIONS

In this section, the efficacy of the neural network estimator is examined in a number of scenarios via simulation. The Quality factor and cantilever stiffness for AFM modeling were chosen according to [23] and the parameters for tip-sample interaction and tip radius are obtained from [24] for two different tip and sample combinations, silicon tip on silicon sample (labeled Si-Si) and silicon tip on polystyrene (labeled Si-PS). The parameters are summarized in Table 2.1. All Simulations were performed in MATLAB using the ode4 solver with fixed step size of 0.0005 in τ .

Table 2.1 AFM parameters.

Symbol	Value
Q	100
k	7.5 Nm^{-1}
R	150 nm
$A_{1\ ,Si\text{-}Si}$	1.3596×10^{-70} $J\,m^6$
$A_{2,\ Si\text{-}Si}$	1.865×10^{-19} $J\,m$
$A_{1\ ,Si\text{-}PS}$	0.838873×10^{-70} $J\,m^6$
$A_{2,\ Si\text{-}PS}$	1.15072×10^{-19} $J\,m$

4.1 SENARIOE 1: NOMINAL PERFORMANCE

In this scenario, the tip and sample materials are assumed to be silicon. The drive signal is $F_{dr}(\tau)=\sin(t)$ resulting in a free amplitude (the tip amplitude when it is far from the sample) of 10.66nm. The sample offset is set to x_s=9.7nm, which results in a relatively light tapping on the sample surface. The basis function centers were chosen as $\bar{x}=9\text{nm}$ and $\delta_j=\left\{-\frac{3}{6},-\frac{2}{6},-\frac{1}{6},0,\frac{1}{6},\frac{2}{6},\frac{3}{6}\right\}$nm. The four sharpnesses parameters in (13)

were used. Thus, the basis vector $\phi(x_1)$ will consist of 4 sharpnesses $\times$ 7 centers =28 RBFs. A number of neural-network estimation gains, σ and *G* were evaluated. As one may expect, larger gains resulted in better estimation error, but also tended to produce a persistent variation in the weighting gains. That is, while the state estimation and force estimation errors were smaller, the weights tended to converge to periodic, non-constant, solutions as the gains were increased. A final choice of gains of $\sigma = 1e-15$ and G=1000I was selected, as this provided the best compromise between force estimation accuracy and constancy of the weights.

Simulation results, shown in Figure 2.4, demonstrate the ability of the neural-network method to estimate the unknown force function. The estimated tip-to-sample force, both as a function of time and as a function of state (Figure 4.a and 4.b, respectively) shows very good agreement and errors in estimation are 0.4% and 1.3% for maximum and minimum force respectively. In addition, estimated weights $\hat{W}$ converge to nearly constant values (there is some updating that continues to occur at the time of impact, located at τ=891 in Figure 4.d.). Convergence of the scheme occurs in approximately 800 normalized seconds, or about 120 tapping cycles.

4.2 SCENARIO 2: CHANGE IN OFFSET

In imaging, the offset of the tip and sample is constantly changing as the sample profile changes. In most imaging, the changes are small, as the AFM feedback system continuously makes adjustments to keep it nearly constant. However, for the tip-to-sample force estimation, even small changes require readjustment of the weighting parameters. In this scenario, we examine the effect of a step change in the tip-to-sample offset.

In this scenario, the offset changes begins at x_s=9.6nm and changes to x_s=9.85nm at $\tau = 900$. All other parameters are kept the same as in the previous section. Results are shown in Figure 2.5. As it can be seen, there is very good agreement between the estimated and actual tip-to-sample force. Error in estimating of minimum force is 6.5% for x_s=9.85nm and 1.9% for x_s=9.6nm and error in estimating the maximum force is about 0.1% for both cases. In part (c), the convergence of weights can be seen also

sudden changes in weights updated at time $\tau = 900$, due to the step change in sample offset at that time are detectable. Convergence to the new weights occurs in about 400 normalized seconds (~65 periods), although notably the convergence to new weights is smoother, showing smaller spikes than the initial convergence.

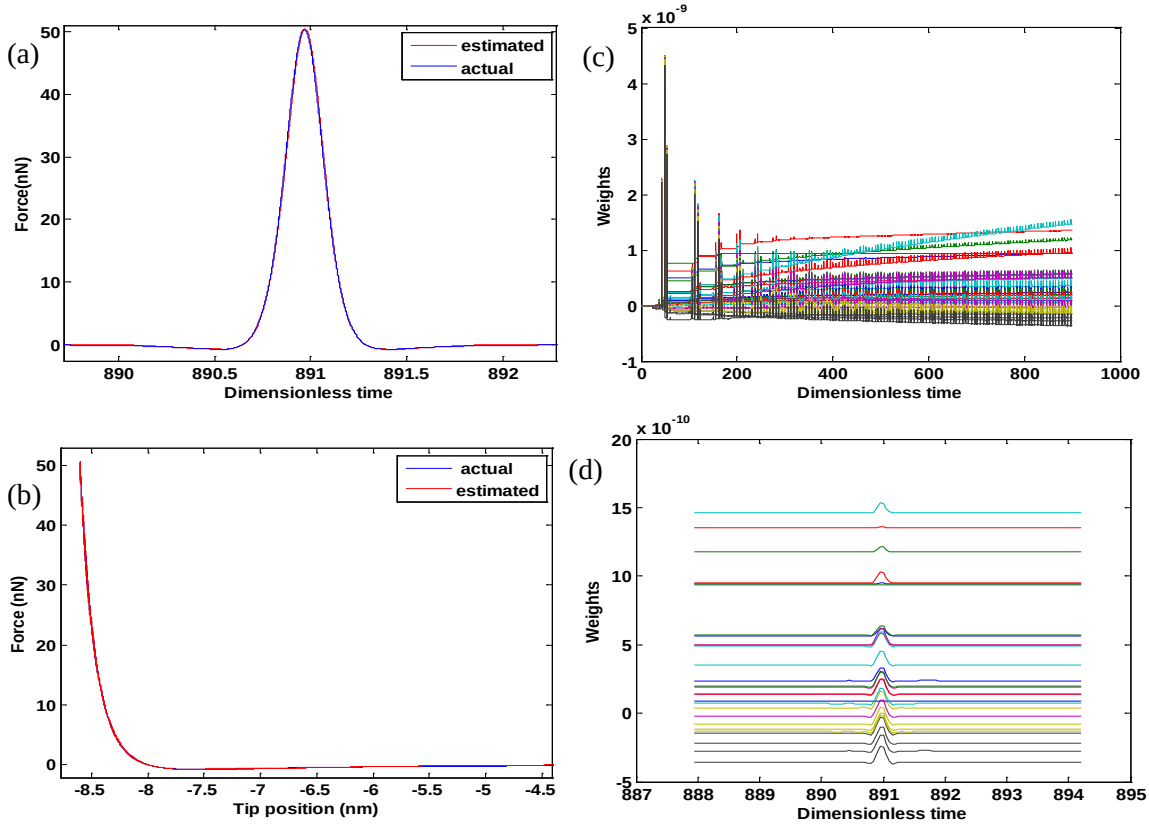

Figure 2.4 Simulation results for Si-Si interaction and sample offset xs=9.7nm. Time is normalized with respect to cantilever's natural frequency such that $\tau = 2\pi$ is one period of oscillation. (a) force vs. time zoomed in at the last full period. (b) force vs. tip displacement. (c) weight update over entire simulation time. (d) weight update zoomed in over last full period.

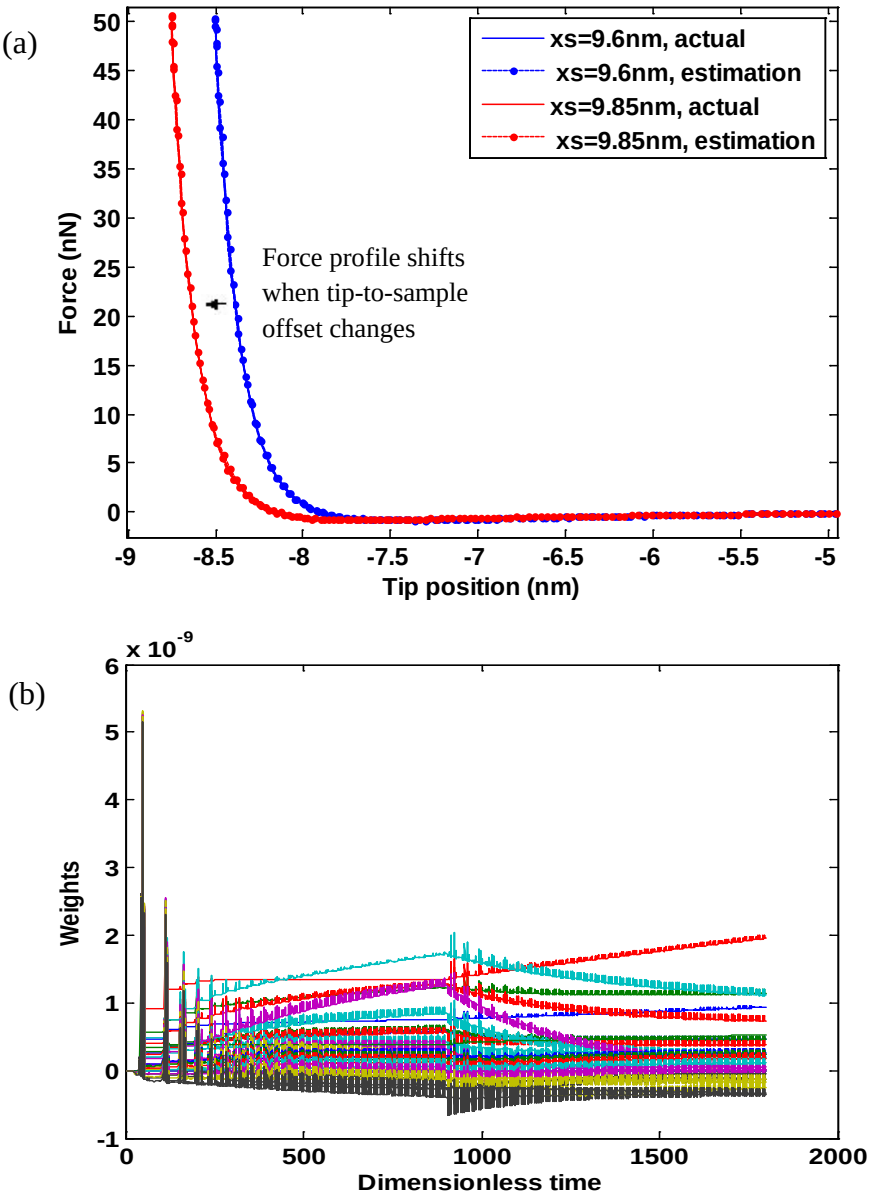

Figure 2.5 Estimated tip-sample force for different sample offsets. (a) force vs. tip position. (b) weight updates.

4.3 SCENARIO 3: CHANGE IN SAMPLE MATERIAL

In this scenario, we consider the problem of identifying the changing force profile as a result of scanning over a new material. The simulation uses a silicon sample for the first 900 simulation time and then changes to a polystyrene sample. The sample offset is held at x_s=9.5 and the remainder of the parameters were the same as in Section 4.1. Estimation results are shown in Figure 2.6. It can be seen from Figure 6 that the method works well in estimating the tip-sample interaction force especially in repulsive regime where the force starts to enter the positive region with a sharp rate of change.

Estimating the maximum force is very good and the error is less than 0.1% for both cases. In addition, it estimates the minimum force with 10% of error for Si-Si interaction and 8.7% of error for Si-PS interaction. The sudden change in material is clearly observed by the sudden change in weights at time 900. Compared to the previous scenario, convergence with a material change occurs much faster, with most weights converging in about 300 normalized seconds (~50 periods).

4.4 SCENARIO 4: MEASUREMENT NOISE

To simulate the effect of measurement noise, a white noise signal with a power of 0.0003 nm^2 is introduced in the measurement. The power of noise is selected such that the level of noise in simulated tip position (x_1) was close to the actual noise level that the authors have observed in the experimental measurements. An offset of x_s=9.5nm and Si-Si interaction were considered.

As already mentioned, large values of G result in faster weight update and better estimation but they are more sensitive to noise and small values of G although they are less sensitive to noise they result in slow weight updates. Thus, there is a tradeoff between noise sensitivity and accuracy in estimation. As a result, value of G lowered to G=100I for the case of noisy measurement which resulted in best compromise between force estimation and noise sensitivity. Simulation Results for this estimation under effect of noise are depicted in Figure 2.7. As it can be seen, although the estimation in time domain is noisy, the force-position profile gives good estimation about actual tip-sample interaction profile.

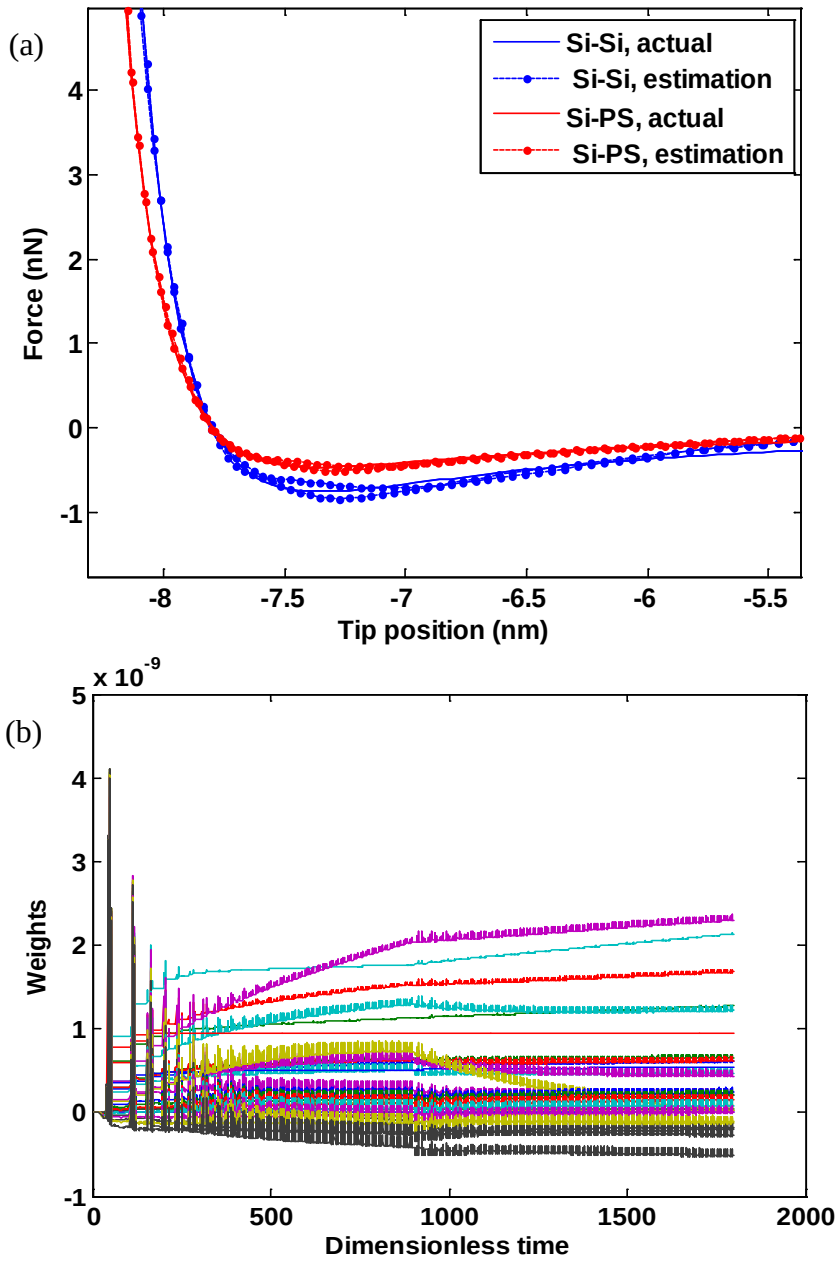

Figure 2.6 Estimated tip-sample force for Si-Si and Si-PS interaction. (a) force vs. tip position. (b) weight updates.

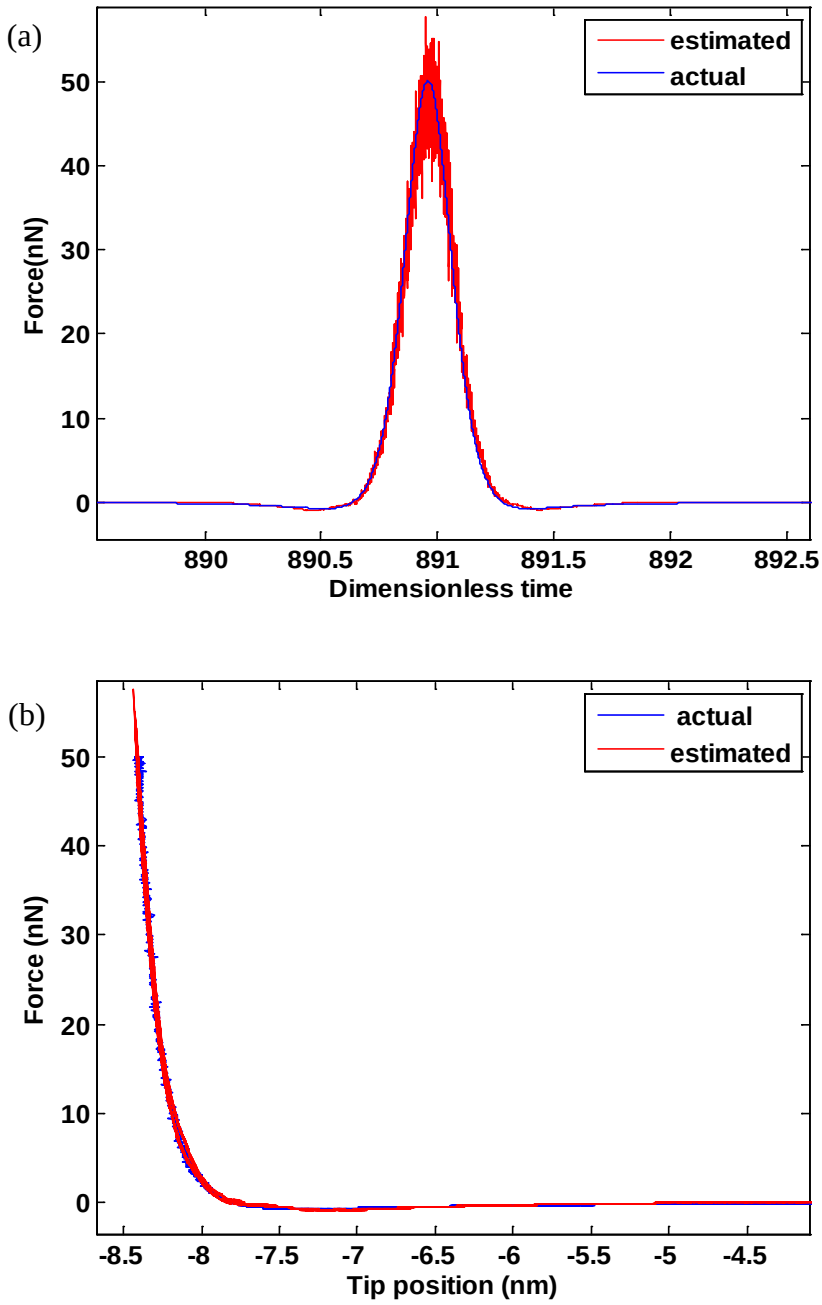

Figure 2.7 Tip-sample force estimation under the effect of noise in states measurement for xs=9.5nm. (a) noisy estimation in force vs. time. (b) force vs. tip position.

5. CONCLUSION

In this paper, a neural network estimation approach is studied to evaluate its potential for estimating the tip-sample interaction in tapping mode AFM. For the method to be applicable in an experimental situation, it should be able to provide good estimation under rapidly changing conditions such as changes in sample offset and material. Simulation results show that this method is plausible, but can be sensitive to the choice of basis functions and weight update parameters. By choosing radial functions with different centers and rates of change, the method was able to estimate the tip-sample force for different sample offsets and materials interactions in simulations.

The investigation revealed some limitations of the neural network approximation approach that must be addressed in future work before the approach can be applied in practice. Firstly, the approach requires full state measurement, but in practice only position is measured. The effect of estimating the velocity, such as with a Kalman filter [27], will be an area of future exploration. Secondly, there may be some challenges in real-time implementation, which will restrict sampling rate and computational complexity. However, the neural network approach is expected to be particularly well suited to these challenges, since neural network can be performed in a parallel processing setup. Finally, the effect of model errors, particularly in assuming a 2^{nd} order oscillator for the cantilever, will need to be evaluated.

REFERENCES

[1] N. Jalili, K. Laxminarayana, "A review of atomic force microscopy imaging systems: application to molecular metrology and biological sciences," Mechatronics, vol. 14, 2004, pp. 907-945.

[2] H. N. Pishkenari, N. Jalili, A. Meghdari, "Acquisition of high-precision images for non-contact atomic force microscopy," Machatronics, vol. 16, 2006, pp. 655-664.

[3] A. S. Paulo, R. Garcia, "High-resolution imaging of antibodies by Tapping-Mode atomic force microscopy," Biophysical J. vol. 78, 2000, pp. 1599-1605.

[4] S. M. Salapaka, M.V. Salapaka, "Scanning probe microscopy," IEEE control system magazine, 2008, pp. 65-83.

[5] R. Garcia, R. Perez, "Dynamic atomic force microscopy methods," Surface Science Reports, vol. 47, 2002, pp. 197-301.

[6] J.N. Israelachvili, *Intermolecular and Surface Forces*, Academic Press, 2nd ed., 1991.

[7] E. Bonaccurso, F. Schönfeld, H.J. Butt, "Electrostatic forces acting on tip and cantilever in atomic force microscopy," Physical Review B vol. 74, 2006, pp. 085413.

[8] A. Sebastian, A. Gannepalli, M.V. Salapaka, "A review of the systems approach to the analysis of dynamics-mode atomic force microscopy," *IEEE transactions on control systems technology*. vol. 15, 2007, pp. 952-959.

[9] G. Schitter, P. Menold, H. F. Knapp, F. Allgowerb, A. Stemmer, "High performance feedback for fast scanning atomic force microscopes," Review of Scientific Instruments, vol. 72, 2001, pp. 3320-3327.

[10] N. Jalili, M. Dadfarnia, D.M. Dawson, "A fresh insight into the microcantilever-sample interaction problem in non-contact atomic force microscopy," Journal of Dynamic Systems, Measurement and Control, vol. 126, 2004, pp.327-335.

[11] S. Crittenden, A. Raman, R. Reifenberger, “Probing attractive forces at the nanoscale using higher-harmonic dynamic force microscopy,” Physical Review B, vol. 72, 2005, pp. 1-13.

[12] S. Hu, S. Howell, A. Raman, R. Reifenberger, M. Franchek. “Frequency domain identification of tip-sample van der Waals interactions in resonant atomic force micro cantilevers,” Journal of Vibration and Acoustics, vol. 126, 2004, pp. 343-351.

[13] R. Garcia, A. San Paulo, “Attractive and repulsive interaction regimes in tapping-mode atomic force microscopy,” Physical Review B, vol. 60, 1999, pp. 4961-4967.

[14] J.R. Lozano and R. Garcia, “Theory of phase spectroscopy in bimodal atomic force microscopy,” Physical Review B, vol. 79, 2009, pp. 014110.

[15] H. Holscher, W. Allers, U. D. Schwartz, R. Wiesendanger, “Determination of tip-sample interaction potentials by dynamic force spectroscopy,” Physical Review Letters, vol. 83, 1999, pp. 4780-4783.

[16] B. Gotsmann, B. Anczykowski, C. Seidel, H. Fuchs, “Determination of tip-sample interaction forces from measured dynamic force spectroscopy curves,” Applied Surface Science, vol. 140, 1999, pp. 314-319.

[17] H. Holscher, “Quantitative measurement of tip-sample interactions in amplitude modulation atomic force microscopy,” Applied Physics Letters, vol. 89, 2006, pp. 123109.

[18] O. Sahin, S. Magonov, C. Su, C. F. Quate, O. Solgaard, “An atomic force microscope tip designed to measure time-varying nanomechanical forces,” Nature Nanotechnology, vol. 2, 2007, pp. 507-513.

[19] O. Sahin, “Time-varying tip-sample force measurements and steady-state dynamics in tapping-mode atomic force microscopy,” Physical Review B, vol. 77, 2008, art. No. 115405.

[20] M. Stark, R. W. Stark, W. M. Heckl, R. Guckenberger. “Inverting dynamic force microscopy: from signals to time-resolved interaction forces,” Applied Physical Sciences, vol. 99, No. 13, 2002, pp. 8473-8478.

[21] R. Padhi, N. Unnikrishnan, S.N. Balakrishnan, “Model-following neuro-adaptive control design for non-square, non-affine nonlinear systems,” IET Control Theory Appl., vol. 1, 2007, pp. 1650-1661.

[22] S. Seshagiri, H. K. Khalil, “Output feedback control of nonlinear systems using RBF neural network,” IEEE Transactions on Neural Networks, vol. 11, No. 1, 2000, pp. 69-79.

[23] R. W. Stark, G. Schitter, A. Stemmer, “Tuning the interaction forces in tapping mode atomic force microscopy,” Physical Review B, vol. 68, 2003.

[24] S. Rutzel, S. I. Lee, A. Raman, “Nonlinear dynamics of atomic-force microscope probes driven in Lennard-Jones potentials,” in *Proc. R. Soc. London*, vol. 459, 2003, pp. 1925-1948.

[23] S. Morita, F.J, Giessibl, R.Wiesendanger, *Noncontact Atomic Force Microscpoy*, Springer, Vol. 2, 2009.

[26] M. H. Hassoum, *Fundamentals of artificial Neural Network*, Cambridge, MA, MIT Press, 1995.

[27] D. R. Sahoo, T. De, M.V. Salapaka, “Observer based imaging for atomic force microscopy,” *Pros. of 44th IEEE Conference on Decision and Control*. 2005, pp. 1185-1190.

II. ESTIMATION OF TIP-SAMPLE FORCE SIGNAL IN TAPPING MODE AFM USING A REPETITIVE CONTROL BASED FILTER

ABSTRACT

Atomic Force Microscopy is one of the most powerful tools for imaging, measuring and manipulating materials at nanometer scale. Among different modes of AFM, tapping mode, in which the oscillating tip approaches and retracts the sample periodically, is most common mode. In this mode, the tip experiences different force regimes, which contain information about the sample topology, material properties and tip geometry. However, measurement of the time-varying tip-sample force signal is challenging in the tapping mode because of the combined dynamic complexities of the cantilever and nonlinear complexity of the tip-sample force. In this paper, considering periodic feature of tapping mode, an approach based on repetitive control is used to design a filter for execrating tip-sample force signal from noisy tip displacement measurements. Design of the filter parts and their parameters are explained and effect of each parameter on force estimation performance is discussed using simulations. Improvement in filter performance by using torsional harmonic cantilevers as the sensor is also presented.

1. INTRODUCTION

The atomic force microscope (AFM) system is now an advanced and useful tool for direct measurements with atomic-resolution and can be employed in a broad spectrum of applications. The applications of atomic force microscopy can be divided in three main areas of imaging, measuring properties and manipulating small structures which are all done at the nanometer scale [1-5]. When the AFM tip scans the surface, it interacts with sample, and various force fields such as van der Waals, electrical, etc. act on the tip of cantilever. These forces, which depend on spatial, geometrical and physical parameters of tip and sample [6], [7], alter the amplitude, frequency and phase of cantilever oscillation. As a result, obtaining these forces reveals good information about sample condition and state of the tip. These information will be of great usage for high-performance controllers [8], [9], high-resolution imaging [10], sample identification and determining tip wearing or contamination [11], [12].

Many researchers have tried to extract tip-sample interaction especially in taping mode AFM. In [13-15] change of amplitude and phase as a function of tip-sample offset are measured to create the tip-sample force function. Utilizing benefits of higher harmonics to improve AFM performance have been a subject of recent works [16], [17]. In one approach utilizing higher harmonics in tip-sample interaction estimation, torsional harmonic cantilever (THC) is designed and torsional rotation of the probe is used to measure time-varying tip-sample forces [18], [19]. Most of the mentioned methods for force extraction relay on steady-state respond of cantilever and require offline or post processing to extract the tip-sample force. Although steady-state measurements may reduce sensitivity to noise, they cannot be efficient in practice due to slow response of probes with high quality factors [20]. One non-steady-state approach constructs tip-sample force estimations from probe displacements applying inverse dynamic of the probe [21]. In another approach, authors try to develop an online estimator using ability of Neural-Network to model unknown functions [22]. However, mentioned non-steady-state methods have the drawback of sensitivity to noise and model uncertainty.

In this paper, a method based on repetitive control (RC) is developed to reconstruct the tip-sample force. RC is well-known to deal with control problems having periodic references and disturbances [23], [24]. Treating the tip-sample force as a periodic disturbance makes force estimation in AFM a good case to utilize RC abilities. A periodic reference-tracking problem with RC is rearranged to a filtering problem where input of filter is probe displacement measurements and output is approximated tip-sample force. The goal of this study is using simulations to evaluate the performance of the presented RC filter to extract tip-sample force in AFM problem. In addition, it is tried to determine effective parameters in design of the filter, tune them, and suggest solutions for performance improvement. The rest of paper is organized as follows. In section 2, a brief AFM model along with assumed tip-sample force model is presented. RC filter structure, design parameters and tuning of them are described in section 3 which is followed by simulation results and discussion in section 4. Next, an improvement solution by applying the RC method on torsional harmonic cantilevers is presented in section 5 and conclusions are given in section 6.

2. MODELING OF AFM AND TIP-SAMPLE FORCE

The AFM dynamics can be modeled as a spring-mass-damper system [1], [8], [23]. Using this, equation of motions of the tip displacement can be obtained by,

$$m\ddot{x} + c\dot{x} + kx = F(x,t)\,, \tag{1}$$

where m is the equivalent cantilever-tip mass, c represents viscous damping and k is the equivalent cantilever spring constant. x is the tip position which is measured from the rest position (Figure 3.1) . $F(x,t)$ is the sum of all forces acting on the tip which are from a dither piezo at the base of cantilever and the tip-sample interaction force,

$$F(x,t) = F_{dr}(t) + F_{ts}(x)\,. \tag{2}$$

For enhancement in analysis and simulation, dynamics are normalized using the dimensionless parameter $2\pi\tau = t\omega$, where $\omega = \sqrt{k/m}$ is the natural frequency. This makes time and frequency normalized with respect to natural frequency of cantilever such that unit of time is one period of oscillation and having frequency of unity means oscillating at natural frequency. Defining the quality factor $Q = m\omega/c$, (1) can be written as,

$$\ddot{x}(\tau) + \frac{2\pi}{Q}\dot{x}(\tau) + (2\pi)^2 x(\tau) = \frac{(2\pi)^2}{k}\left(F_{ts} + F_{dr}\right). \tag{3}$$

Different models have been used to represent the tip-sample interaction force. Using Lennard-Jones model based on [6], [25], the tip-sample force is given by,

$$F_{ts}(x) = +\frac{A_1 R}{180(x+x_s)^8} - \frac{A_2 R}{6(x+x_s)^2}\,, \tag{4}$$

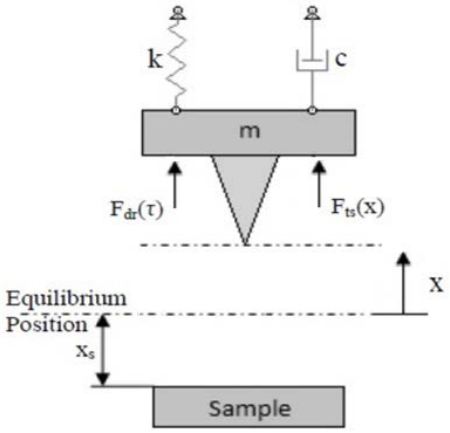

Figure 3.1 SDOF model of AFM.

where coefficients A_1 and A_2 are the Hamaker constants and related to tip and sample material [25]. The gap between the sample and rest position of the tip is x_s and R is the tip radius. The drive force F_{dr} is typically a sine wave near the resonant frequency of cantilever to provide maximum excitation. It should be noted that here we use Lennard-Jones model only to represent the actual tip-sample force in simulations, and to extract the tip-sample force approximation no information from this model is used.

3. FILTER DESIGN USING REPETITIVE CONTROL METHOD

3.1 STRUCTURE OF FILTER

In this section, design of a repetitive control (RC) based filter to extract the tip-sample force in tapping mode AFM is presented. Repetitive control methods are well known to deal with systems with periodic behavior [23], [24]. The goal here is not to make the system to track a specific reference. The objective is to estimate the tip-sample force using information from measured tip position and AFM model. The basic concept is to feed the measured output to the inverse of AFM model to obtain the input force. However, the presence of noise in the output measurements and structure of the inverse model of AFM, which amplifies the effect of noise, makes extracting the force signal very difficult.

Here we rearrange the tracking structure to a filter structure such actual tip displacement can be extracted from noisy AFM measurements. Next, by feeding clean tip displacement to inverse model of AFM, the force can be obtained. A simple repetitive control structure corresponding to our problem has been presented in part (a) of Figure 3.2, where $\hat{G}(s)$ represents the plant dynamics transfer function and $L(s)$, $Q(s)$ are for enhancing the guarantee of stability of closed loop and will be designed [24]. X represents AFM measurement, n is measurement noise and e^{-sT} is the time delay with T representing the period of the first harmonic in the reference. Again, one should note that our reference here is not a clean command signal like regular tracking problems. Here, $X+n$ forms our pseudo reference and $\hat{X}$ forms the estimated or filtered output. Tracking structure has been rearranged to a filtering structure as shown in part (b), where $\hat{h}$ is the estimated force. Part (c) shows how the filter is implemented and part (d) shows the transfer function $H(s)$ or the RC filter. Here we consider $L(s)$ having the following form

$$L(s) = \alpha \hat{G}^{-1}(s) F(s), \quad 0 < \alpha < 1, \tag{5}$$

where α is a learning rate and $F(s)$ an appropriate lowpass filter. Using that, the transfer function for RC filter is given by,

$$H(s)=\frac{\alpha F(s)Q(s)e^{-sT}}{1+\alpha F(s)Q(s)e^{-sT}-Q(s)e^{-sT}}. \tag{6}$$

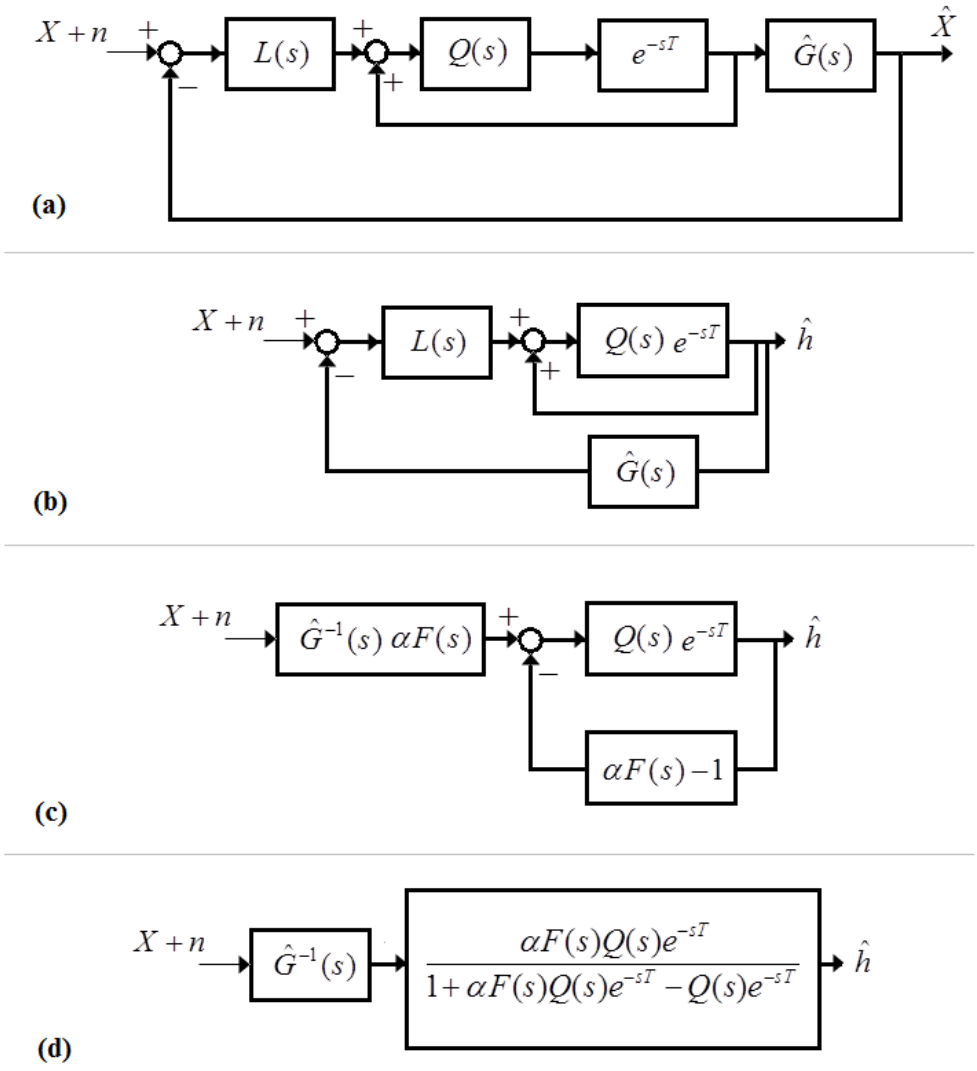

Figure 3.2 Rearrangements of RC tracking problem to RC filter for force estimation. (a) tracking structure (b) filtering structure (c) implementing structure (d) RC filter transfer function.

By designing $F(s)$ and $Q(s)$ as appropriate lowpass filters with magnitude close to unity before their cutoff frequency, response of $H(s)$ can be approximated as follow.

- At harmonics:

$$s = j\frac{2\pi}{T}k,\ k = 0,1,2,\ldots \Rightarrow e^{-sT} = 1,\ Q(s) \approx F(s) \approx 1 \Rightarrow |H(s)| \approx 1 \tag{7}$$

- Between harmonics:

$$s = j\frac{2\pi}{T}(k+\frac{1}{2}),\ k = 0,1,2,\ldots \Rightarrow e^{-sT} = -1,\ Q(s) \approx F(s) \approx 1 \Rightarrow |H(s)| \approx \frac{\alpha}{2-\alpha} \tag{8}$$

This is desired since filter will pass signal at harmonics, which has good information, and attenuates signal between harmonics, which contains noise and has no information. An example frequency response of $H(s)$ with $\alpha = 0.01$ has been illustrated in Figure 3.3 .

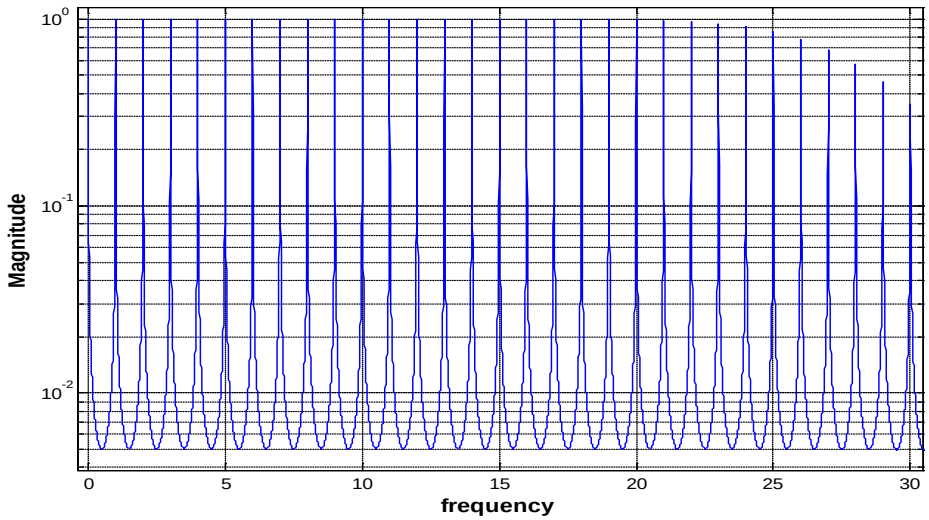

Figure 3.3 An example of $H(s)$ frequency response with learning rate of $\alpha = 0.01$ and $Q(s)$ having a cutoff at 25 normalized frequency.

3.2 DESIGN OF FILTER

In this section, main parts of RC filter, their parameters, and how to find the range of those parameters are discussed. It is tried to explain these such that one can understand how to change this parameters based on difference data acquisition devises, AFM cantilevers, and performance objectives (i.e. speed or accuracy). As shown in previous section, lowpass filters $F(s), Q(s)$ and the parameter α are main tools for designing the RC filter. These can be designed and tuned, as long as stability of overall system is held. It can be shown by small gain theorem that the closed-loop system is stable if the following condition holds for all frequencies (in discrete-time domain it will be up to Nyquist frequency) [23],

$$\left\| Q(s)(1-\hat{G}(s)L(s)) \right\|_{\infty} = \left\| Q(s)(1-\alpha F(s)) \right\|_{\infty} < 1. \tag{9}$$

3.2.1 Design of *F(s)*. The main goal of $F(s)$ is for implementation propose since the inverse of $\hat{G}(s)$ is not implementable alone. Thus, $F(s)$ was chosen as a lowpass filter with cutoff of ω_F and same order of $\hat{G}(s)$ as below,

$$F(s) = \frac{\omega_F^2}{s^2 + 2\varsigma\omega_F + \omega_F^2}, \quad (\varsigma = 0.7). \tag{10}$$

Damping ratio $\varsigma = 0.7$ is chosen to prevent any sharp pick in frequency response of $F(s)$. To avoid interfering with $Q(s)$, ω_F is set as high as possible but the limit for ω_F is determined by half of sampling frequency. To determine that limit, one should consider data acquisition system sampling rate and the AFM cantilever excitation frequency. In our case, data acquisition system has a sampling frequency of 100*MHz* and AFM cantilevers work below 300*kHz*. This, results in almost 330 samples per period. Since in dimension less domain our system has period of unity ($T = 1$), the sampling frequency (SF) in simulation must be 330 samples/period or 330Hz or lower. One the other hand, it should be picked such that integer multiples of time step (*dt*) can cover one period. Thus, sampling frequency of SF=250 (normalized) was selected for simulation which results in

time step of $dt = 0.004$ in normalized domain. This determines that upper limit for ω_F can be $\frac{250}{2} = 125$. In our simulations, $\omega_F = 80$ was selected.

3.2.2 Design of *Q*(*s*). $Q(s)$ is also a lowpass filter with cutoff of ω_Q which determines the cutoff of the filter *H*(s). In this paper, Butterworth filters were used for design of $Q(s)$. However, they were not implemented directly and some modifications were applied to enhance the performance. Due to the phase in $Q(s)$, applying that directly will introduce a phase shift between actual and extracted tip-sample force signal. To address this problem, zero-phase FIR filter was made using a Butterworth filter and following these steps:

1. Using $Q(z)$ (discrete form of $Q(s)$), calculate the impulse response $q[n]$ for $(n = 1, 2, ..., N)$ where *N* is the number of samples in one period *T*.
2. convolve q[n] and its flipped backward version $q'[n]$ to obtain zero-phase filter as below,

$$Q_{zp} = q[n] * q'[n]. \tag{11}$$

Parameters effective in shaping $Q(s)$ are its cutoff ω_Q, filter type, and filter order. Generally, the cutoff for $Q(s)$ must be less than $F(s)$ to provide stability. On the other hand, it should be high enough to cover appropriate number of harmonics to capture tip-sample force. As a result, frequency content of the tip-sample force signal can be used to determine number of required harmonics to reconstruct the tip-sample force and hence select ω_Q. Frequency spectrum (FFT) of tip-sample force signal simulating free amplitude oscillations, soft tapping, and hard tapping showed 25-40 number of harmonics are required to capture tip-sample force. This suggests a range of 25-40 (normalized frequency) for ω_Q.

3.2.3 Learning Rate Parameter α . Effect of parameter α on filter performance can be analyzed by considering the transfer function from the noise in measurement (*n*) to the error in force estimation due to noise (e_h) as given in by following equation

$$\frac{e_h}{n} = \frac{\alpha F(s)Q(s)e^{-sT}}{1+\alpha F(s)Q(s)e^{-sT} - Q(s)e^{-sT}} \hat{G}^{-1}(s). \tag{12}$$

Assuming high bandwidth for $Q(s)$ and $F(s)$ (i.e. $Q(s) \approx F(s) \approx 1$), poles of (12) can be approximated by setting denominator equal to zero.

$$1+(\alpha-1)e^{-sT} = 0 \Rightarrow s^* = \frac{\ln(1-\alpha)}{T} + j\frac{2\pi}{T}k, \;\; k = 0,1,2,\ldots. \tag{13}$$

Thus, the time constant of filter will be

$$\tau_H = -\frac{T}{\ln(1-\alpha)} \approx \frac{T}{\alpha} \;\; (for \;\alpha << 1). \tag{14}$$

It can be seen from (12)-(14) that α is a tradeoff between noise reduction and convergence time.

4. SIMULATION RESULTS

Having determined effective parameters and their range theoretically in previous section, performance of RC filter in tip-sample force approximation is investigated here using simulations. The objective is to study how performance of RC filter changes by changing design parameters. Furthermore, it is tired to see how these parameters should be changed with regard of each other, if there is an optimum value, and how the performance can be improved.

4.1 EFFECT OF α ON FILTER PERFORMANCE

As it was shown in previous part, α is a trade of between noise reduction and conversance rate. To check this effect, a zero mean Gaussian noise with variance of $(1e-10)^2$ was added to simulated position measurements. This variance was chosen such that it generates the similar level of noise in simulated measurements as authors have observed in experimental measurements. Simulations were run for $\alpha = 0.1, 0.02, 0.004$ while $Q(s)$ was selected as a 4^{th} order Butterworth lowpass filter with cutoff $\omega_Q = 40$. Norm of error between actual and approximated tip-sample force in last 10 cycles was used as a criteria to measure RC filter performance.

Results show the ability of RC filter in approximating the tip-sample force signal and it can captures maximum force with less than 10% error although it cannot approximate the minimum force (Figure 3.4). In addition, confirms the idea that while smaller α reduces the noise effect (lower error norm), it increases the convergence time dramatically and this is almost proportional to inverse of α as mentioned in(14). These have been summarized in Table 3.1.

Table 3.1 Effect of α on RC filter force approximation performance.

α	0.1	0.02	0.004
Error norm (N)	2.18e-7	7.85e-8	6.41e-8
Convergence duration (cycles)	140	620	3000

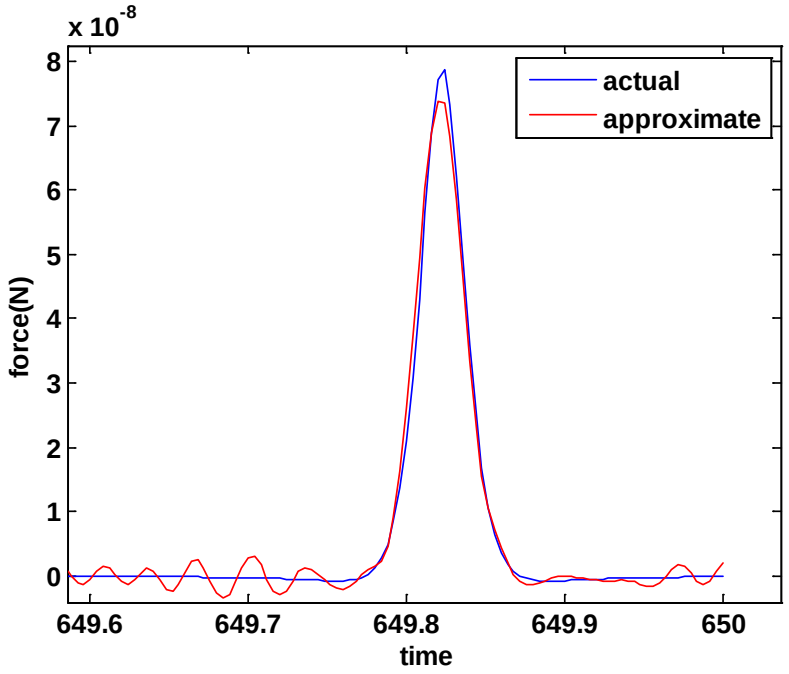

Figure 3.4 Force approximation using RC filter ($Q(s)$ is 4th order Butterworth, $\omega_Q = 40$ and $\alpha = 0.02$).

4.2 EFFECT OF $Q(s)$ CUTOFF FREQUENCY AND ORDER

As mentioned, other parameters that can be changed in RC filter are ω_Q and order of $Q(s)$. Effect of ω_Q was investigated by keeping the other parameters fixed and picking various values for ω_Q. Since FFT analysis showed up to 40 harmonics are required to

capture the tip-sample force, values of $\omega_Q = 30, 35, 40, 45$ were selected for simulation. For the next case, the order of $Q(s)$ was changed and 2^{nd}, 4^{th}, 6^{th} , and 8^{th} order Butterworth lowpass filters were chosen, while $\omega_Q = 40$ and $\alpha = 0.02$ were kept unchanged. While it is expected that increasing the cutoff will allow filter to capture more harmonics and hence better force approximation, result in Figure 3.5 shows that increasing the cutoff does not improve the performance necessarily and there is an optimal value for ω_Q . The same can be concluded for increasing the order of filter (Figure 3.6). One reason that can explain this is that although increasing cutoff will allow passing more harmonics, it will pass more noise also. As a result, if signal to noise ratio (SNR) of signal becomes less than unity for frequencies below ω_Q , filter will pass more noise rather than signal which decreases the performance in force estimation.

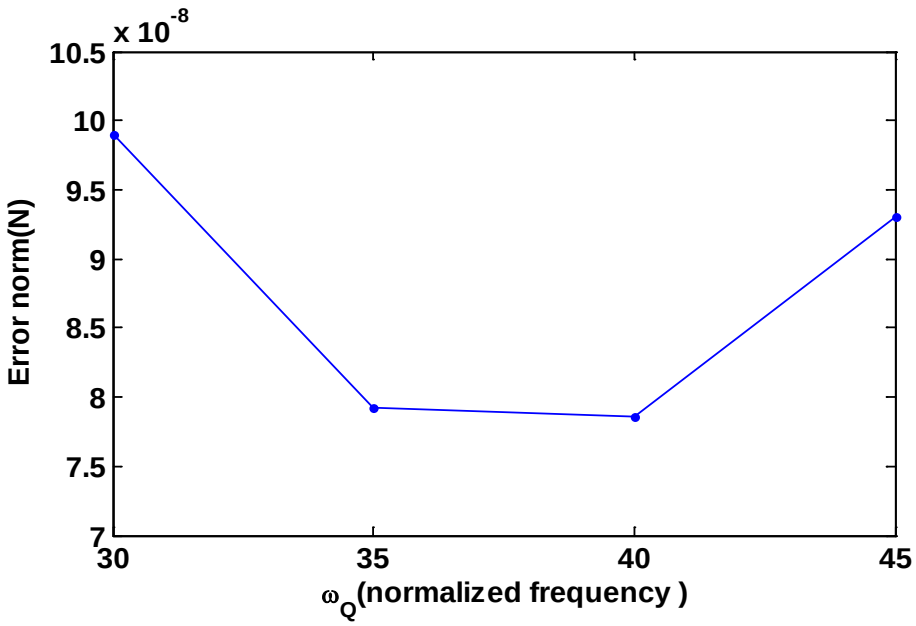

Figure 3.5 Effect of changing ω_Q on force estimation performance. ($Q(s)$ is 4^{th} order Butterworth, and $\alpha = 0.02$).

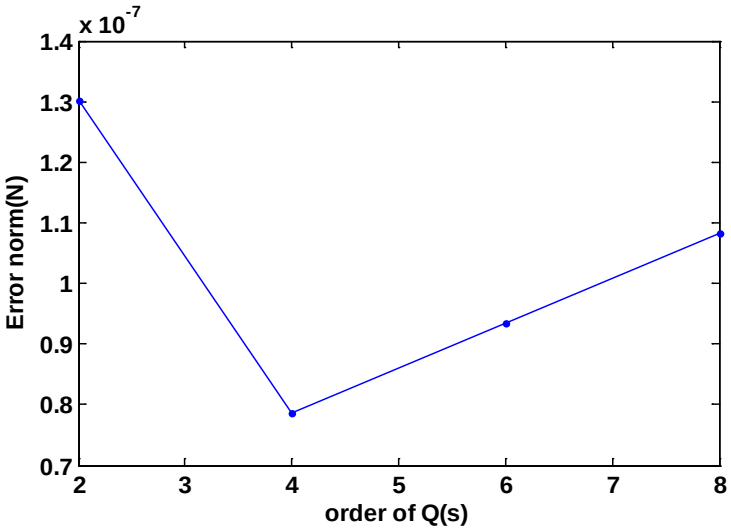

Figure 3.6 Effect of changing $Q(s)$ order on force estimation performance. ($\omega_Q = 40Hz$ and $\alpha = 0.02$).

The assumed reason was verified by calculating the signal to noise ratio (SNR) at each frequency as below

$$SNR_k = \frac{\left\| a_k e^{j\phi_k} \right\|}{\left\| \hat{a}_k e^{j\hat{\phi}_k} - a_k e^{j\phi_k} \right\|}, \tag{15}$$

where $a_k, \phi_k, \hat{a}_k, \hat{\phi}_k$ represent magnitude and phase for FFT of simulated $\hat{X}$ for actual (with noise) and modeled (without noise) AFM output respectively and *k* denotes the harmonic number. This was repeated for different values of α and crossing frequencies at which SNR value fall below unity were recorded and tabulated in Table 2 . This provides an idea for frequency at which the RC filter should start to roll off. Performance of RC filter with $Q(s)$ having cutoffs around crossing frequencies was studied in the next step. Results, illustrated in Figure 7, show that setting the cutoff of $Q(s)$ at crossing frequencies does not provide the best performance. This is due to fact that $Q(s)$ starts

rolling off (magnitude becomes less that unity) about 5Hz before the cutoff. Thus, the ω_Q should be set 5-10 above the crossing frequency. This trend can be seen in Figure 3.7. In addition, it illustrates an important fact that in design of RC filter, parameters α and ω_Q cannot be picked independently and as α is increased ω_Q should be decreased to prevent passing noise.

Table 3.2 Corresponding crossing frequencies (normalized) for various values of α.

α	0.1	0.05	0.01
Crossing frequency	25	25	29

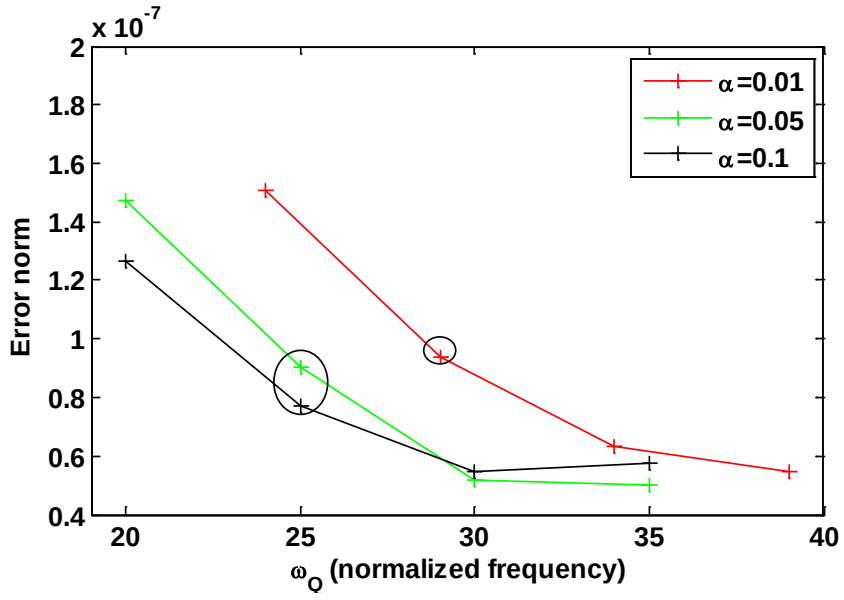

Figure 3.7 Performance of RC filter when ω_Q is set around crossing frequencies (crossing frequencies according to Table 1 are encircled).

5. IMPROVING RC PERFORMANCE USING THC

Utilizing higher harmonics in atomic force microscopy and engineering cantilevers for these purposes have been subject of various works [16-18]. Thus, authors believe using a sensor (cantilever) with enhanced higher harmonic excitation structure (i.e., THC) will address the problem of low SNR in bending cantilevers and improve the performance of RC filter. This idea is explored here by investigating performance of RC filter to approximate tip-sample force using THC as a sensor in AFM.

5.1 MODELING OF TORSIONAL HARMONIC CANTILEVER

In THC, the tip is placed with an offset from the long axis of cantilever [18]. Here, THC was modeled by adding a massless torsional element with moment of inertia of J and torsional spring constant K_θ to the previous mass-spring-damper as illustrated in Figure 3.8. Considering the free body diagram and assuming no mass for the torsional element, the equation of motion will be

$$\begin{cases} m\ddot{x}(t) + c\dot{x}(t) + kx(t) = F_{ts} + F_{dr} \\ J\ddot{\theta}(t) + c_\theta\dot{\theta}(t) + k_\theta\theta(t) = F_{ts} \times d \end{cases}. \tag{16}$$

Using corresponding quality factors, angular frequencies, dimensionless time $2\pi\tau = \omega t$, and natural frequency ratio $r = \dfrac{\omega}{\omega_T}$, equation (16) can be reformed as below,

$$\begin{cases} \ddot{x}(\tau) + \dfrac{2\pi}{Q}\dot{x}(\tau) + (2\pi)^2 x(\tau) = \dfrac{(2\pi)^2}{k}\left(F_{ts} + F_{dr}\right) \\ r^2\ddot{\theta}(\tau) + \dfrac{2\pi r}{Q_T}\dot{\theta}(\tau) + (2\pi)^2\theta(\tau) = \dfrac{(2\pi)^2}{k_\theta}F_{ts} \times d \end{cases}. \tag{17}$$

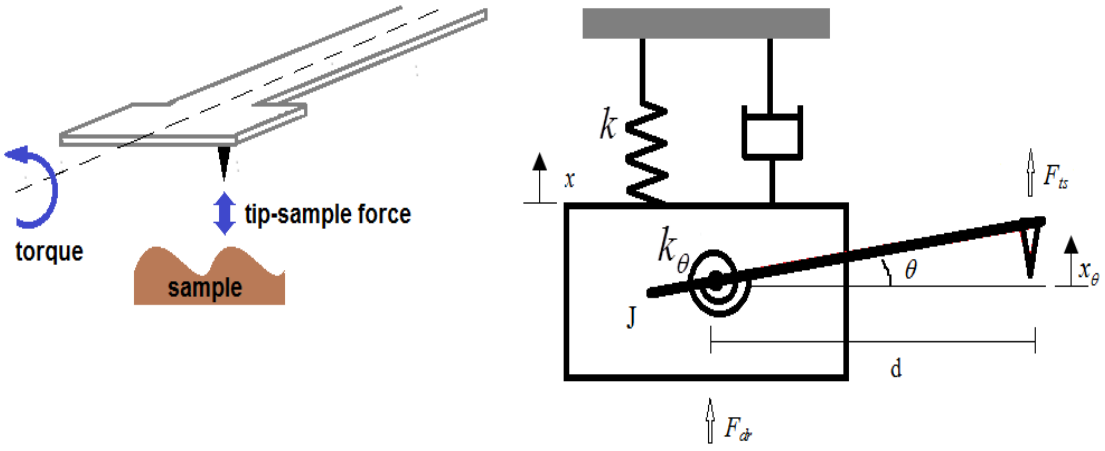

Figure 3.8 Schematic view of THC and simplified model of that by adding a massless torsional element.

By introducing scaled torsional spring constant $k_T = \frac{k_\theta}{d^2}$, and displacement due to rotation $x_\theta = d\,\theta$, second equation in (17) can be rearranged to have final set of equations of motion for THC as below,

$$\begin{cases} \ddot{x}(\tau) + \dfrac{2\pi}{Q}\dot{x}(\tau) + (2\pi)^2 x(\tau) = \dfrac{(2\pi)^2}{k}\left(F_{ts} + F_{dr}\right) \\ r^2\,\ddot{x}_\theta(\tau) + \dfrac{2\pi r}{Q_T}\dot{x}_\theta(\tau) + (2\pi)^2 x_\theta(\tau) = \dfrac{(2\pi)^2}{k_T}F_{ts} \end{cases} . \tag{18}$$

Here, we assumed that torsional displacement could be measured separately from bending displacement. In addition, to be close to values given in [18], we assumed numerical values given in Table 3.3 for simulating THC model.

Table 3.3 THC model parameters.

symbol	value
Q_T	400
k_T	550 N/m
r	16.2

5.2 RC FILTER PERFORMANCE IN COMBINATION WITH THC

Comparing frequency spectrum of THC and regular bending cantilever as shown in Figure 3.9, confirms that torsional harmonic cantilever is a better candidate for tip-sample force estimation using RC filter since it has stronger higher harmonic excitations. To verify that, THC model was considered as the model of AFM. Torsional cantilevers usually have higher quality factors which result in a sharper pick in their frequency response near the natural frequency. Thus, in selecting methods which are used to convert continuous-time models to discrete-time, one should select the one that provides the most similar frequency response to the continuous-time system. Figure 3.10 shows bode plots of discretized $L(s)$ using different MATLAB methods which has been magnified near the torsional natural frequency. As it can be seen, only *"matched"* method provides the best match and *"foh"* and *"tustin"* methods do not match the continuous model in either magnitude or frequency. These mismatches will cause wrong harmonics to appear in approximated tip-sample force signal.

Performance of RC filter in torsional and bending mode was compared by considering same RC filter design and parameters. For considering more challenging scenario, the noise level was amplified by factor of three. Simulations were run for two cases of learning rate $\alpha = 0.1$ and $\alpha = 0.01$. Results, as depicted in Figure 3.11 and Figure 3.12, indicate significant improvement of RC filter performance in combination with torsional harmonics cantilevers and confirm the suggested idea of using torsional harmonic cantilevers. Looking at RC filter force approximation performance using

bending and torsional cantilever, and also considering the values of α, it can be concluded that using THC allows selecting higher values for α without compromising the performance accuracy. This will also result in faster tip-sample force estimation.

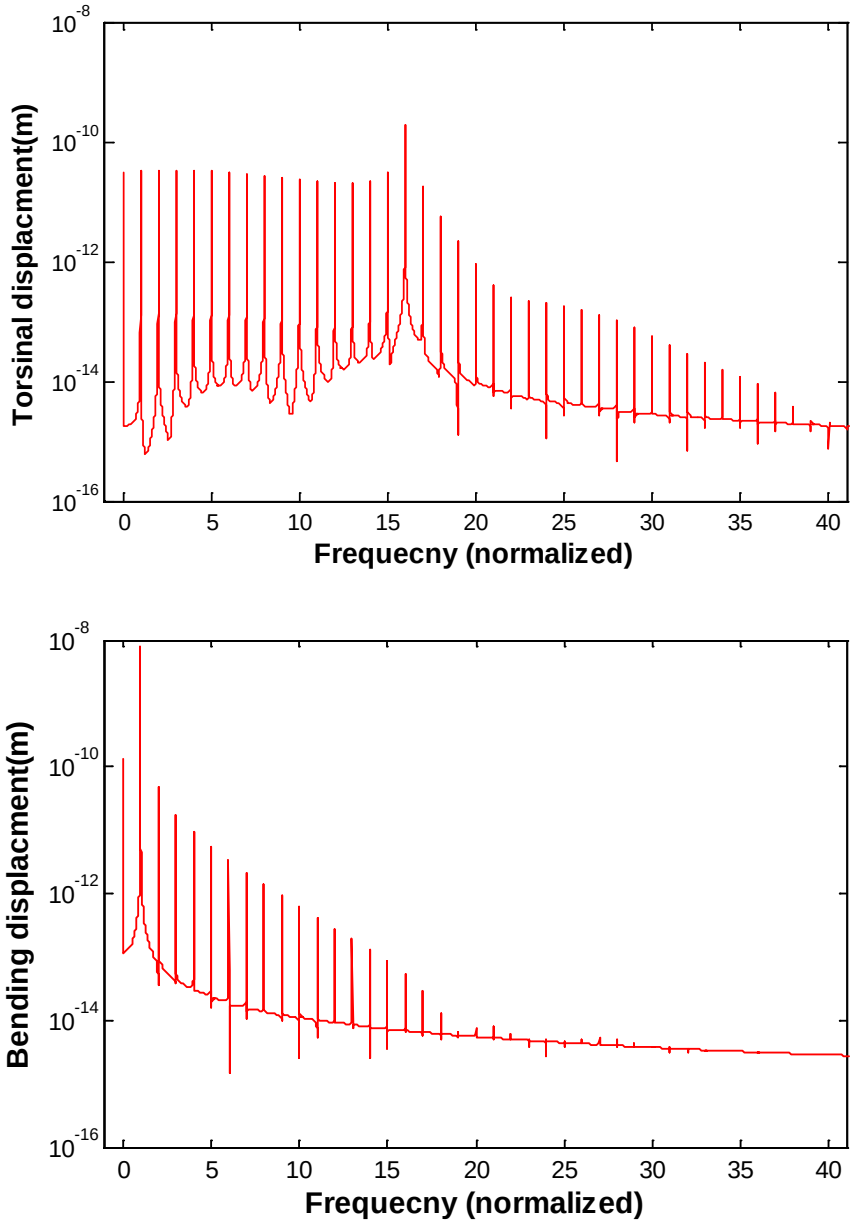

Figure 3.9 Frequency spectrum for (top) THC (bottom) regular bending cantilever.

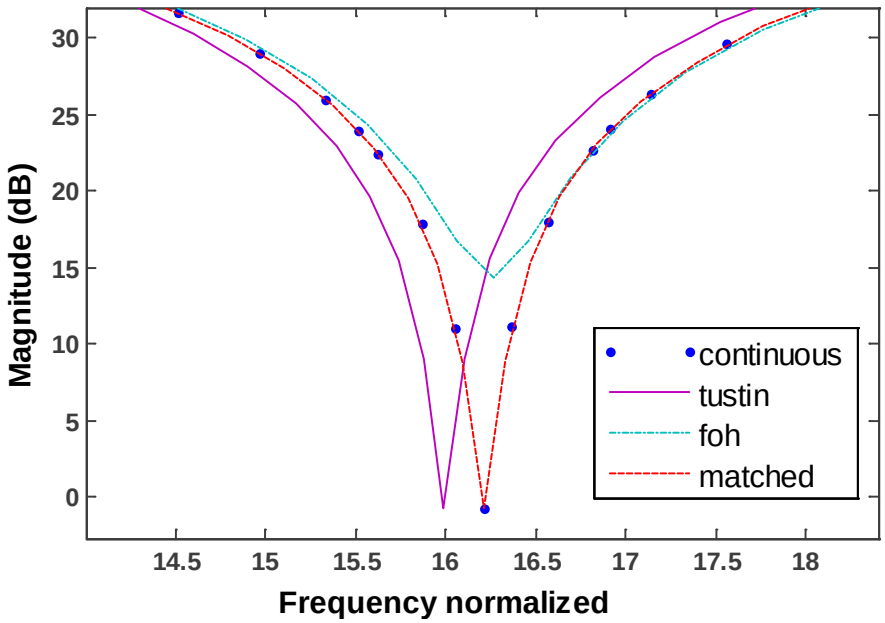

Figure 3.10 Bode plot of $L(s)$ using MATLAB's "tustin", "first order hold" and "matched" discretization methods (the plot is zoomed in near the resonance peak).

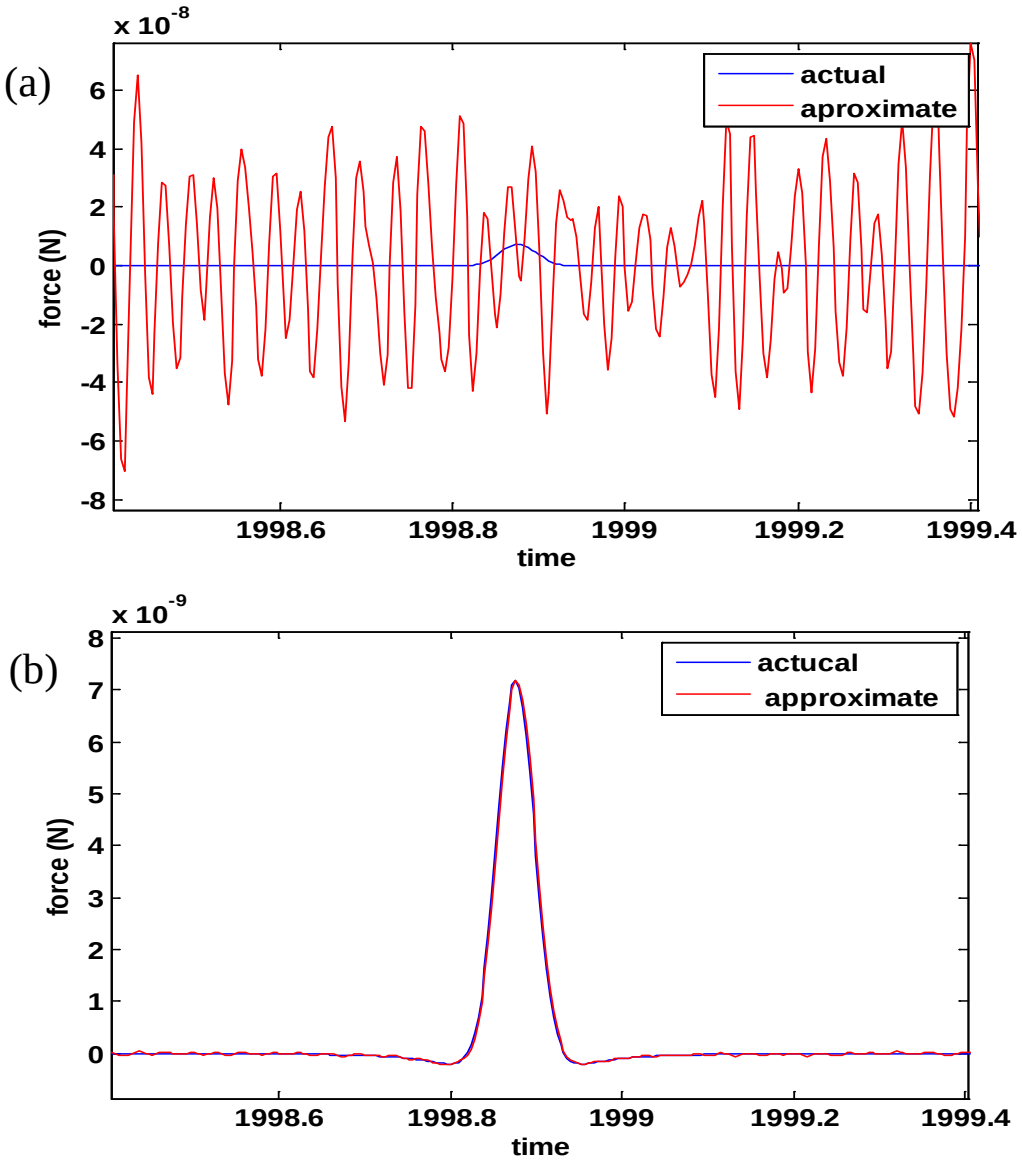

Figure 3.11 Comparison of RC filter tip-sample force approximation using (a) regular bending cantilever (b) THC ($\alpha = 0.1$ for both cases).

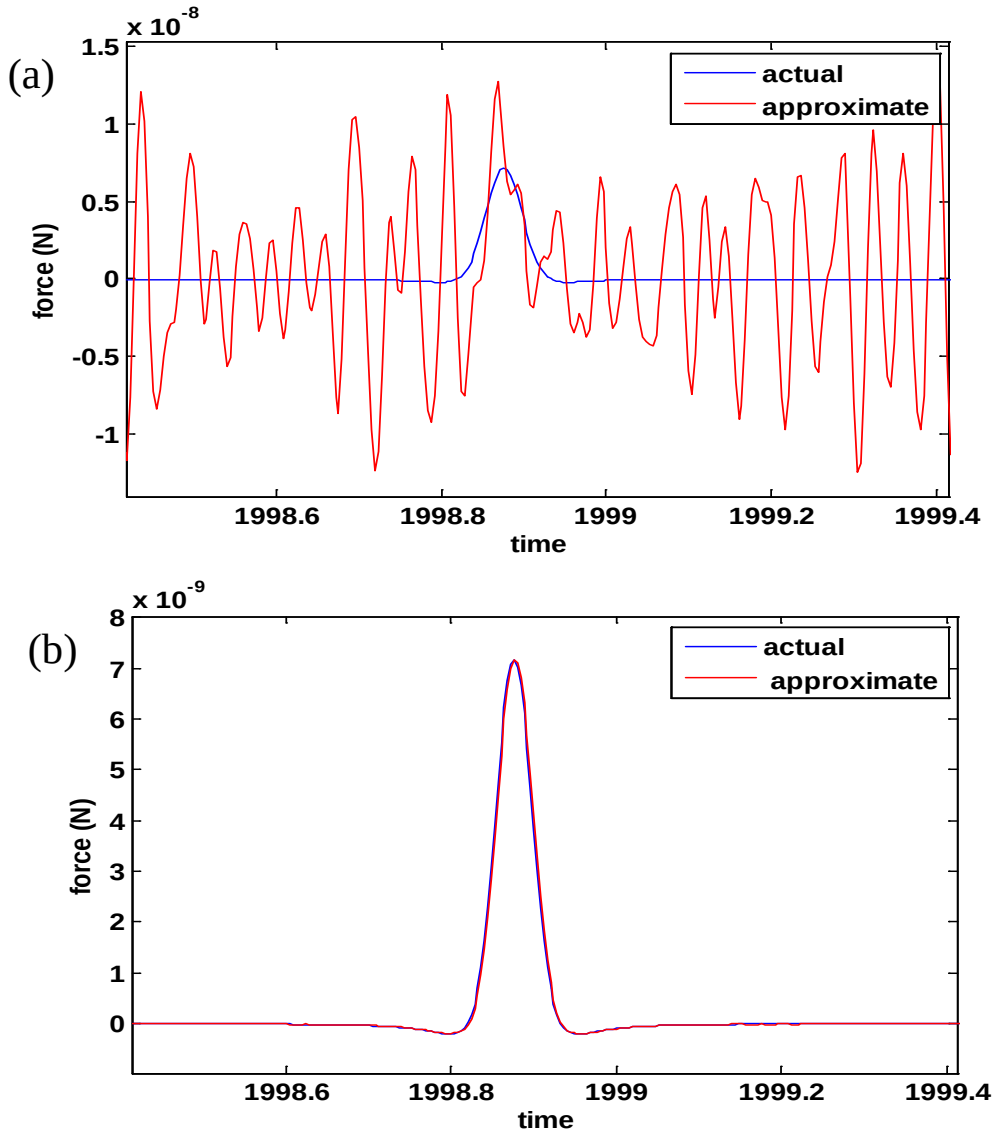

Figure 3.12 Comparison of RC filter tip-sample force approximation using (a) regular bending cantilever (b) THC ($\alpha = 0.01$ for both cases).

6. CONCLUSION

In this article, an approach based on repetitive control to extract the tip-sample force in taping mode AFM was presented. Filter design parameters and tuning them to satisfy stability and improving performance were explained. Simulation results for regular AFM cantilevers, where bending displacement of probe is measured, showed that there was a tradeoff between noise cancelation and the convergence time. In addition, it was found out that although in theory increasing filter cutoff frequency may allow better tip-sample force signal reconstruction, in practice and in presence of noise there is a limit and increasing the cutoff above that will pass more noise than signal.

To address that problem and improving the performance, utilizing a probe with better frequency content at higher harmonics (torsional harmonic cantilevers) was suggested. Results confirmed application of RC filter in combination with THC. Simulation results showed a significant improvement in tip-sample force estimation. These improvements were better accuracy in force approximation and faster convergence in comparison with the case of using regular bending probes.

In addition, investigations revealed that in implementing the RC filter in discrete-time domain, consideration must be taken to match the model and physical system as close as possible. This shows the sensitivity of this RC method to uncertainties in AFM model and more studies on dealing with uncertainties and estimating them adaptively will enhance RC filter performance. Challenges in implementing the RC filter digitally especially is systems with high sampling rates [26] must be explored before the approach can be applied in practice. Finally, combining advantages of RC filter in noise cancelation and abilities of neural-network methods in approximating unknown functions can be a subject of future researches to obtain tip-sample force profile.

REFERENCES

[1] N. Jalili, K. Laxminarayana, “A review of atomic force microscopy imaging systems: application to molecular metrology and biological sciences,” Mechatronics, vol. 14, 2004, pp. 907-945.

[2] H.N. Pishkenari, N. Jalili, A. Meghdari, “Acquisition of high-precision images for non-contact atomic force microscopy,” Machatronics, vol. 16, 2006, pp. 655-664.

[3] A. S. Paulo, R. Garcia, “High-resolution imaging of antibodies by Tapping-Mode atomic force microscopy”, Biophysical J. vol. 78, 2000, pp. 1599-1605.

[4] S. M. Salapaka, M.V. Salapaka, “Scanning probe microscopy,” IEEE control system magazine, 2008, pp. 65-83.

[5] R. Garcia, R. Perez, “Dynamic atomic force microscopy methods,” Surface Science Reports, vol. 47, 2002, pp. 197-301.

[6] J.N. Israelachvili, Intermolecular and Surface Forces, Academic Press, 2nd ed., 1991.

[7] E. Bonaccurso, F. Schönfeld, H.J. Butt, “Electrostatic forces acting on tip and cantilever in atomic force microscopy,” Physical Review B vol. 74, 2006, pp. 085413.

[8] A. Sebastian, A. Gannepalli, M.V. Salapaka, “A review of the systems approach to the analysis of dynamics-mode atomic force microscopy,” IEEE transactions on control systems technology. vol. 15, 2007, pp. 952-959.

[9] G. Schitter, P. Menold, H. F. Knapp, F. Allgowerb, A. Stemmer, “High performance feedback for fast scanning atomic force microscopes,” Review of Scientific Instruments, vol. 72, 2001, pp. 3320-3327.

[10] N. Jalili, M. Dadfarnia, D.M. Dawson, “A fresh insight into the microcantilever-sample interaction problem in non-contact atomic force microscopy” Journal of Dynamic Systems, Measurement and Control, vol. 126, 2004, pp.327-335.

[11] S. Crittenden, A. Raman, R. Reifenberger, “Probing attractive forces at the nanoscale using higher-harmonic dynamic force microscopy,” Physical Review B, vol. 72, 2005, pp. 1-13.

[12] S. Hu, S. Howell, A. Raman, R. Reifenberger, M. Franchek. “Frequency domain identification of tip-sample van der Waals interactions in resonant atomic force micro cantilevers,” Journal of Vibration and Acoustics, vol. 126, 2004, pp. 343-351.

[13] H. Holscher, W. Allers, U. D. Schwartz, R. Wiesendanger, “Determination of tip-sample interaction potentials by dynamic force spectroscopy” Physical Review Letters, vol. 83, 1999, pp. 4780-4783.

[14] B. Gotsmann, B. Anczykowski, C. Seidel, H. Fuchs, “Determination of tip-sample interaction forces from measured dynamic force spectroscopy curves,” Applied Surface Science, vol. 140, 1999, pp. 314-319.

[15] H. Holscher, “Quantitative measurement of tip-sample interactions in amplitude modulation atomic force microscopy” Applied Physics Letters, vol. 89, 2006, pp. 123109.

[16] M. Loganathan, D. A. Bristow, “Bi-harmonic cantilever design for improved measurement sensitivity in tapping-mode atomic force microscopy,” Review of Scientific Instruments, vol. 85, 2014, pp. 043703.

[17] S. Sadewasser, G. Villanueva, J. A. Plaza, “Modified atomic force microscopy cantilever design to facilitate access of higher modes of oscillation,” Review of Scientific Instruments, vol. 77, 2006, pp. 073703.

[18] O. Sahin, S. Magonov, C. Su, C. F. Quate, O. Solgaard, “An atomic force microscope tip designed to measure time-varying nanomechanical forces,” Nature Nanotechnology, vol. 2, 2007, pp. 507-513.

[19] O. Sahin, “Time-varying tip-sample force measurements and steady- state dynamics in tapping-mode atomic force microscopy,” Physical Review B, vol. 77, 2008, art. No. 115405.

[20] D. R. Sahoo, A. Sebastian, M. V. Salapaka, “Harnessing the transient signals in atomic force microscopy,” International Journal of Robust Nonlinear Control, vol.15, 2005, pp. 805–820.

[21] M. Stark, R. W. Stark, W. M. Heckl, R. Guckenberger. “Inverting dynamic force microscopy: from signals to time-resolved interaction forces,” Applied Physical Sciences, vol. 99, No. 13, 2002, pp. 8473-8478.

[22] A. Toghraee, D. A. Bristow, S.N. Balakrishnan , ”Estimation of tip-sample interaction in tapping mode AFM using a neural-network approach,” American Control Conference, 2012, pp. 3222-3227.

[23] R. W. Longman, “Iterative learning and repetitive control for engineering practice,” International Journal of Control, vol. 73, No. 10, 200, pp. 930-954.

[24] M. Steinnuch, “Repetitive control for systems with uncertain period-time,” Automatica, vol. 38, 2002, pp. 2103-2109.

[25] S. Rutzel, S. I. Lee, A. Raman, “Nonlinear dynamics of atomic-force microscope probes driven in Lennard-Jones potentials” in *Proc. R. Soc. London,* vol. 459, 2003, pp. 1925-1948.

[26] H. L. Chang, T. C. Tsao, “An efficient fixed-point realization of inversion based repetitive control,” American Control Conference, 2013, pp. 5968-5973.

SECTION

2. CONCLUSIONS AND FUTURE WORK

The objective of this research was developing methods to extract tip-sample force profile in tapping mode AFM using different approaches. Modeling, analysis, and results of this research were presented in sections “Paper I” and “Paper II”.

In first part, a neural network estimation approach was studied to evaluate its potential for estimating the tip-sample interaction in tapping mode AFM. It was shown that is able to provide good estimation under rapidly changing conditions such as changes in sample offset and material which happen in real practical situations. Simulation results show that this method is plausible, but can be sensitive to the choice of basis functions and weight update parameters. By choosing radial functions with various centers and sharpnesses, the method was able to estimate the tip-sample force for different sample offsets and materials interactions in simulations.

The investigation revealed some limitations of the neural network approximation approach that must be addressed in before the approach can be applied in practice. Firstly, the approach requires full state measurement, but in practice, only position is measured. This problem can be addressed by either using Kalman filter or modified versions of the applied neural-network e, which uses only output measurement. Secondly, there may be challenges in real-time implementation, which will restrict sampling rate and computational complexity. However, the neural network approach is expected to be particularly well suited to these challenges, since neural network can be performed in a parallel processing setup.

In second part, an approach based on repetitive control to extract the tip-sample force in taping mode AFM was presented. It was shown periodic nature of signals in tapping mode AFM makes RC a good candidate to be applied in force approximation problem. Design of filter parameters and tuning them to satisfy stability and improving performance were explained. Simulation results for regular AFM cantilevers, where bending displacement of probe is measured, demonstrated that there was a tradeoff between noise cancelation and the convergence time of the filter. In addition, it was

found out that although in theory increasing filter cutoff frequency may allow better tip-sample force signal reconstruction, in practice and in presence of noise there is link between the learning rate parameter α and cutoff frequency of filter and they cannot be selected independently. Observations also revealed that using regular bending cantilevers as sensors prevent filter from fast force estimation due to low SNR at higher harmonics.

To address that problem and improving the performance, utilizing a probe with better frequency content at higher harmonics (torsional harmonic cantilevers) was suggested and results confirmed application of RC filter in combination with THC. Simulation results showed a significant improvement in tip-sample force estimation. These improvements showed themselves as better accuracy in force approximation and faster convergence in comparison with the case of using regular bending probes.

In addition, it was found out that in implementing the RC filter in discrete-time domain, consideration must be taken in discretizing method to match the model and physical system as close as possible. Challenges in implementing the RC filter digitally especially is systems with high sampling rates must be explored before the approach can be applied in practice. Both methods require accurate enough cantilever model to reconstruct the tip-sample force and considering SDOF models and other uncertainties in the AFM model and parameters need to be evaluated.

Finally, combining advantages of RC filter in noise cancelation and abilities of neural-network methods in approximating unknown functions can be a subject of future researches to obtain tip-sample force profile.

VITA

Alireza Toghraee was a Mechanical Engineering M.S. student in Mechanical Engineering Department at the Missouri University of Science and Technology (Missouri S&T). In August 2015, he received his M.S. Mechanical Engineering from Missouri University of Science and Technology. He was born in Tehran, Iran. He Attended Tabriz University in Tabriz from 2001 to 2006 and received his B.Sc. degree in Mechanical Engineering. In 2006 he was granted to study Tarbiat Modares University in Tehran and earned his M.S. degree in Mechanical Engineering working on the vibration and dynamics of carbon nanotubes under effect of shock to design nano switches. During his M.S. program in Missouri University of Science and Technology, he worked on projects to determine and estimate tip-sample force in tapping mode AFM, he explored Neural-Network, and Repetitive Control approaches to approximate the force.